DdcA antagonizes a bacterial DNA damage checkpoint

Peter E. Burby, Zackary W. Simmons, Lyle A. Simmons*

Department of Molecular, Cellular, and Developmental Biology, University of Michigan, Ann Arbor, MI 48109, United States.

*Corresponding author

LAS: Department of Molecular, Cellular, and Developmental Biology, University of Michigan, Ann Arbor, Michigan 48109-1055, United States. Phone: (734) 647-2016, Fax: (734) 647-0881

E-mail: lasimm@umich.edu

Running Title: DdcA inhibits a DNA damage checkpoint

Abstract

Bacteria coordinate DNA replication and cell division, ensuring that a complete set of genetic material is passed onto the next generation. When bacteria encounter DNA damage or impediments to DNA replication, a cell cycle checkpoint is activated to delay cell division by expressing a cell division inhibitor. The prevailing model for bacterial DNA damage checkpoints is that activation of the DNA damage response and protease mediated degradation of the cell division inhibitor is sufficient to regulate the checkpoint process. Our recent genome-wide screens identified the gene *ddcA* as critical for surviving exposure to a broad spectrum of DNA damage. The *ddcA* deletion phenotypes are dependent on the checkpoint enforcement protein YneA. We found that expression of the checkpoint recovery proteases could not compensate for *ddcA* deletion. Similarly, expression if *ddcA* could not compensate for the absence of the checkpoint recovery proteases, indicating that DdcA function is distinct from the checkpoint recovery step. Deletion of *ddcA* resulted in sensitivity to *yneA* overexpression independent of YneA protein levels or stability, further supporting the conclusion that DdcA regulates YneA through a proteolysis independent mechanism. Using a functional GFP-YneA we found that DdcA inhibits YneA activity independent of YneA localization, suggesting that DdcA may regulate YneA access to its target. These results uncover a regulatory step that is important for controlling the DNA damage checkpoint in bacteria, and suggests that the typical mechanism of degrading the checkpoint enforcement protein is insufficient to control the rate of cell division in response to DNA damage.

Author Summary

All cells coordinate DNA replication and cell division. When cells encounter DNA damage, the process of DNA replication is slowed and the cell must also delay cell division. In bacteria, the process has long been thought to occur using two principle modes of regulation. The first, is RecA coated ssDNA transmits the signal of DNA damage through inactivation of the repressor of the DNA damage (SOS) response regulon, which results in expression of a cell division inhibitor establishing the checkpoint. The second principle step is protease mediated degradation of the cell division inhibitor relieving the checkpoint. Recent work by our lab and others has suggested that this process may be more complex than originally thought. Here, we investigated a gene of unknown function that we previously identified as important for survival when the bacterium *Bacillus subtilis* is exposed to DNA damage. We found that this gene negatively regulates the cell division inhibitor, but is functionally distinct from the checkpoint recovery process. We provide evidence that this gene functions as an antagonist to establishing the DNA damage checkpoint. Our study uncovers a novel layer of regulation in the bacterial DNA damage checkpoint process challenging the longstanding models established in the bacterial DNA damage response field.

Introduction

The logistics of the cell cycle are of fundamental importance in biology. All organisms need to control cell growth, DNA replication, and the process of cell division. In bacteria the initiation of DNA replication is coupled to growth rate and the cell cycle [1-4]. Bacteria also regulate cell division in response to DNA replication status through the use of DNA damage checkpoints [5, 6]. The models for the DNA damage response (SOS) were developed based on studies of

Escherichia coli and subsequently extended to other bacteria. In this model, DNA damage results in perturbations to DNA replication and the accumulation of ssDNA [7]. The recombinase RecA is loaded onto ssDNA [8-12], and the resulting RecA/ssDNA nucleoprotein filament induces the SOS response by activating auto-cleavage of the transcriptional repressor LexA [13]. LexA inactivation results in increased transcription of genes involved in DNA repair and the DNA damage checkpoint [14-18]. The DNA damage checkpoint is established by relieving the LexA dependent repression of a cell division inhibitor that enforces the checkpoint by blocking cell division [19-22]. Once the checkpoint is established, the delay in cytokinesis provides the cell with enough time to complete DNA replication, thereby ensuring a complete and accurate copy of the chromosome is provided to both daughter cells. Over several decades of study, this overarching model has been consistently demonstrated among bacteria that contain a RecA and LexA dependent DNA damage checkpoint mechanism [5, 23].

Where the DNA damage response varies between bacteria is in the mechanism that enforces and alleviates the checkpoint. In *E. coli* and closely related Gram-negative bacteria, the checkpoint is enforced by SulA, which is a cytoplasmic protein that acts by directly inhibiting formation of the FtsZ ring at mid cell [20, 24-27]. In many other bacteria the checkpoint is enforced by a small membrane binding protein [21, 28-31]. In *Caulobacter crescentus*, the small membrane proteins SidA and DidA inhibit cell division through direct interactions with components of the essential cell division complex known as the divisome [30, 31]. In other bacteria the exact mechanism of checkpoint enforcement remains unclear. In the Gram-positive bacterium *Bacillus subtilis*, the checkpoint enforcement protein YneA is a small protein containing a transmembrane domain as well as a LysM domain. A previous study found that several amino acids on one side of the transmembrane alpha helix are important for function,

which led the authors to suggest that YneA may also interact with a component of the divisome [22]. The same study also suggested full length YneA is the active form, and that the transmembrane domain alone is not sufficient for activity [22]. The mechanism by which YneA enforces the checkpoint is still unknown.

The mechanism of relieving the DNA damage checkpoint has only been identified in two bacterial species, *E. coli* and *B. subtilis*. Despite the checkpoint mechanisms functioning in different cellular contexts, the strategy for checkpoint recovery is remarkably similar between these two organisms. In *E. coli,* Lon protease is the major protease responsible for degrading SulA [32-34], and the protease ClpYQ appears to play a secondary role [35-37]. In *B. subtilis*, there are two proteases YlbL, which we rename here to DdcP (DNA damage checkpoint recovery protease) and CtpA that degrade YneA [38]. In the case of DdcP and CtpA, the former seems to be the primary protease in minimal media, however during chronic exposure to DNA damage in rich media both proteases are important and they can functionally replace each other when overexpressed [38]. DdcP and CtpA are not regulated by DNA damage [38], suggesting that the proteases act as a buffer to YneA accumulation. Thus, in order for the checkpoint to be enforced both proteases must be saturated. Following repair of damaged DNA, LexA represses expression of YneA and the remaining YneA is cleared by DdcP and CtpA allowing cell division to proceed.

Although the DNA damage checkpoint in bacteria is well understood, it is becoming clear that the process is more complex than the models developed thus far. Work from Goranov and co-workers demonstrated that the initiation protein and transcription factor DnaA regulates *ftsL* levels in response to DNA replication perturbations, which contributes to cell filamentation [39]. Further, our recent report identified several genes not previously implicated in genome

maintenance or cell cycle control to be critical for surviving chronic exposure to a broad spectrum of DNA damage [38]. We identified genes involved in cell division and cell wall synthesis as well as genes of unknown function that rendered the deletion mutants sensitive to DNA damage [38]. To understand how the DNA damage response in bacteria is regulated, we investigated the contribution of one of the unstudied genes *ddcA* (formerly *ysoA*, see below) in the DNA damage response. We report that DdcA antagonizes YneA action through a proteolysis independent mechanism. This finding represents a novel regulatory node controlling the DNA damage checkpoint in bacteria.

Results

Deletion of *ddcA* (*ysoA*) results in sensitivity to DNA damage

We recently published a set of genome wide screens using three distinct classes of DNA damaging agents, uncovering many genes that have not been previously implicated in the DNA damage response or DNA repair [38]. One gene that conferred a sensitive phenotype to all three agents tested was *ysoA*, which we rename here to DNA damage checkpoint antagonist (*ddcA*). DdcA is a protein that is predicted to have three tetratrichopeptide repeats (Fig 1A), which are often involved in protein-protein interactions, protein complex formation, and virulence mechanisms in bacteria [40]. In order to better understand the mechanism of the DNA damage response in *B. subtilis*, we investigated the contribution of DdcA. To begin, we tested the sensitivity of the *ddcA* deletion to DNA damage. Deletion of *ddcA* resulted in sensitivity to mitomycin C (MMC) an agent that causes DNA crosslinks and bulky adducts; [41, 42] and phleomycin a peptide that forms double and single strand DNA breaks [43, 44]. We found that expression of P_{xyl}-*ddcA* from an ectopic locus (*amyE)* was sufficient to complement deletion of

ddcA with or without inducing expression using xylose (Fig 1B). We conclude that deletion of *ddcA* results in a *bona-fide* sensitivity to DNA damage.

DNA damage sensitivity of *ddcA* deletion is dependent on *yneA* and independent of nucleotide excision repair.

We asked how DdcA functions in the DNA damage response. Our observation that a *ddcA* deletion allele results in sensitivity to several DNA damaging agents is similar to the result of deleting the checkpoint recovery proteases. Given that our prior study [38] showed that DNA damage phenotypes in checkpoint recovery protease mutants depend on the checkpoint enforcement protein, *yneA*, we asked whether the same was true for *ddcA*. We found that in the *ddcA* deletion background, deletion of *yneA* was indeed capable of rescuing sensitivity to MMC (Fig S1). We also tested for a genetic interaction with nucleotide excision repair, reasoning that the absence of nucleotide excision repair would result in increased *yneA* expression and increased sensitivity in the *ddcA* deletion. Indeed, deletion of *uvrAB*, genes coding for components of nucleotide excision repair [45], resulted in hypersensitivity to MMC (Fig S1). These data, together with the initial observation of general DNA damage sensitivity, rule out a role for DdcA in nucleotide excision repair and suggest that DdcA functions in some aspect of regulating cell division during the DNA damage response.

DdcA functions independent of DNA damage checkpoint recovery proteases

Based on the observation that sensitivity to DNA damage in a Δ*ddcA* mutant was rescued by deletion of *yneA*, similar to our observations with the checkpoint recovery proteases [38], we hypothesized that DdcA could function within the checkpoint recovery pathway. This hypothesis predicts that deletion of *ctpA* or *ddcP (ylbL)* would be epistatic to deletion of *ddcA*. In contrast,

we observed that deletion of *ddcA* in a *ctpA* or *ddcP* mutant resulted in increased sensitivity to MMC (Fig 2A). To test this hypothesis further, we tested the effect of deletion of *ddcA* in a Δ*ddcP*, Δ*ctpA* double mutant on MMC sensitivity. We found that deletion of *ddcA* resulted in increased MMC sensitivity relative to the double protease mutant (Fig 2B), suggesting that DdcA functions independently of both DdcP and CtpA. We then asked if *yneA* was responsible for the phenotype of Δ*ddcA* in the absence of the checkpoint recovery proteases. Strikingly, we found that the sensitivity of the triple mutant was mostly dependent on *yneA*, but at elevated concentrations of MMC, there was a slight but reproducible difference when *ddcA* was deleted in the Δ*ddcP*, Δ*ctpA*, Δ*yneA::loxP* mutant background (Fig 2B). Taken together, with these data we suggest that DdcA functions independently of checkpoint recovery proteases, but negatively regulates the checkpoint enforcement protein YneA.

In our previous study we found that the checkpoint recovery proteases could substitute for each other [38], we therefore asked if DdcA could function in place of the checkpoint recovery proteases or if the proteases could function in place of DdcA. To test this idea, we overexpressed *ddcP* and *ctpA* in a Δ*ddcA* mutant and found that neither protease could rescue a *ddcA* deletion phenotype (Fig 3A). We also found that expression of *ddcA* in the double protease mutant could not rescue the MMC sensitive phenotype (Fig 3B). Further, expression of *ddcP* or *ctpA* were each able to partially complement the phenotype of the triple mutant, but expression of *ddcA* had no effect at higher concentrations of MMC (Fig 3B). As a control, we verified that overexpression of *ddcA* using high levels of xylose (0.5% xylose) could complement a Δ*ddcA* mutant (Fig S2). We also found that at lower concentrations of MMC, expression of *ddcA* could rescue the *ddcA* deficiency of the triple mutant resulting in a phenotype indistinguishable from the double protease mutant (Fig 3C). Given that DdcA cannot substitute for DdcP and CtpA, we

considered the possibility that YneA protein levels increased in the absence of *ddcA*. We tested this by monitoring YneA protein levels following MMC treatment and after recovering from MMC treatment for two hours. Deletion of *ddcA* alone did not result in a detectable difference in YneA protein levels compared to WT (Fig S3). Further, deletion of *ddcA* in the double protease mutant also did not result in an increase in YneA protein levels relative to the double protease mutant with *ddcA* intact (Fig S3). With these data we conclude that DdcA has a function distinct from that of the checkpoint recovery proteases. We also conclude that DdcA does not regulate YneA protein abundance.

***ddcA* deletion results in sensitivity to *yneA* overexpression independent of YneA stability**

Prior work established that overexpression of *yneA* resulted in growth inhibition [21, 22]. Indeed, we found that the double checkpoint recovery protease mutant was considerably more sensitive than the wild type strain to *yneA* overexpression [38]. Given that DdcA has a function distinct from DdcP and CtpA and that YneA protein levels did not increase when *ddcA* was deleted, we initially hypothesized that a *ddcA* mutant would not be sensitive to *yneA* overexpression. In contrast, we found that the Δ*ddcA* mutant was more sensitive to *yneA* overexpression than WT (Fig 4A), and that deletion of *ddcA* in the double protease mutant background resulted in exquisite sensitivity to *yneA* overexpression (Fig 4A). We asked whether YneA protein levels changed under these conditions, and again there was no detectable difference when *ddcA* was deleted alone or when combined with the double protease mutant (Fig 4B). We also considered the possibility that DdcA could affect the stability of YneA rather than the overall amount. To test this idea, we performed a translation shut-off experiment and monitored YneA stability over time. We induced expression of *yneA* in the double protease mutant with and without *ddcA* and blocked translation. We found that YneA protein abundance decreased at a similar rate

regardless of whether *ddcA* was present (Fig 4C). We conclude that DdcA negatively regulates YneA independent of protein stability.

DdcP and CtpA are membrane anchored with extracellular protease domains

The observation that DdcA and the checkpoint recovery proteases have distinct functions led us to ask where these proteins are located within the cell. YneA is a membrane protein with the majority of the protein located extracellularly [22]. We hypothesized that proteases DdcP and CtpA should be similarly localized if YneA is a direct substrate. We used the transmembrane prediction software TMHMM [46] and found that both DdcP and CtpA were predicted to have an N-terminal transmembrane domain, as reported previously [47]. We tested this prediction directly using a subcellular fractionation assay [48]. We found that DdcP and CtpA were present predominantly in the membrane fraction (Fig 5A). DdcP is predicted to have a signal peptide cleavage site [47], however, we did not detect DdcP in the media (Fig 5A), suggesting that DdcP is membrane anchored and not secreted. The membrane topology of DdcP and CtpA could put the protease domains inside or outside of the cell (Fig 5B). To determine their location we used a protease sensitivity assay [Fig 5B; 49]. Cells were treated with lysozyme, followed by incubation with proteinase K. We found that DdcP and CtpA were digested by proteinase K, but the intracellular protein DnaN was not (Fig 5C). In control reactions we added Triton X-100 to disrupt the plasma membrane, which rendered all three proteins susceptible to proteinase K (Fig 5C). To verify that the N-terminal transmembrane domain is required for DdcP and CtpA to be extracellular we created N-terminal truncations (Fig 5D), and repeated the proteinase K sensitivity assay. With these variants, DdcP and CtpA should be locked inside the cell, and indeed, both N-terminal truncations were now resistant to proteinase K similar to DnaN (Fig 5E).

We conclude that DdcP and CtpA are tethered to the plasma membrane through N-terminal transmembrane domains and their protease domains are extracellular (Fig 5B, left panel).

DdcA is an intracellular protein

YneA has a transmembrane domain and has previously been shown to be localized to the plasma membrane [22], and we now show that DdcP and CtpA are membrane anchored as well. To better understand how DdcA limits YneA activity, we asked where DdcA was located. We were unable to find DdcA detected in any previous proteomic experiments that interrogated cytosolic or extracellular proteins [50-52]. The fact that DdcA has not been detected using proteomics is not surprising given that DdcA is likely to be present at low levels because complementation of the *ddcA* deletion allele occurs from the P_{xyl} promoter in the absence of inducer (Fig 1). Also, the secretome of *B. subtilis* was analyzed using bioinformatics and reported [47], however, DdcA was not predicted to be secreted through the canonical secretion mechanisms. Therefore, we turned to other bioinformatics prediction programs to determine if DdcA would be targeted to the membrane or secreted. We used several programs to predict the subcellular location of DdcA [46, 53-55]. The transmembrane prediction programs TMHMM [46] and TMpred [53] did not predict a transmembrane domain in DdcA. The program SecretomeP, which predicts the likelihood that a protein is secreted through a non-canonical mechanism [54], rendered a "SecP score" of 0.068654, which is well below the threshold of 0.5 for secreted proteins and more similar to cytosolic proteins. Similarly, the program PSORTb (v3.0.2), which predicts the subcellular location of proteins [55], predicted that DdcA would reside in the cytosol. Taken together, DdcA is predicted to be present in the cytosol.

In order to experimentally determine the location of DdcA, we generated GFP fusions to the N- and C-termini of DdcA. We tested whether GFP-DdcA and DdcA-GFP were functional by assaying for the ability to complement a *ddcA* deletion. We found that GFP-DdcA was capable of complementing a *ddcA* deletion in the presence or absence of xylose for induced expression (Fig 6A), similar to that observed with untagged DdcA (Fig 1). In contrast, DdcA-GFP was partially functional, because complete complementation was only observed when expression of *ddcA-gfp* was induced using xylose, but not in the absence of xylose (Fig 6A). As a control we asked if we could detect free GFP via Western blotting using GFP specific antiserum. We did not detect the fusion proteins in lysates if expression was not induced using xylose. We found that both DdcA fusions were detectable at their approximate molecular weight of 67.6 kDa when induced with 0.05% xylose (Fig 6B), though we did see that the C-terminal fusion had a slight increase in mobility (Figure 6B, arrowhead). Importantly, we did not detect a significant band near 25 kDa, the approximate size of GFP (Fig 6B), suggesting that GFP is not cleaved from DdcA. We did detect a very faint proteolytic fragment (Fig 6B, arrow) that seemed to occur during the lysis procedure. After establishing the functionality and integrity of the GFP-DdcA fusion we chose to visualize DdcA localization via fluorescence microscopy.

To compare the background fluorescence of *B. subtilis* cells, we imaged WT (PY79) cells under the same conditions as the GFP-DdcA fusion strain. We found a low level of background fluorescence in WT cells, and when a line scan of fluorescence intensity through a cell was plotted there was a very slight increase in signal intensity in the span between the fluorescent membrane peaks (Fig 6C). The GFP-DdcA fusion was detectable throughout the cell at very low levels in the absence of xylose induction, with the intensity being slightly greater than WT cells (Fig 6C). We then imaged cells under conditions in which *gfp-ddcA* expression was induced with

0.05% xylose. This experiment shows that GFP-DdcA was found throughout the cytosol, and the scan of fluorescence intensity was significantly greater than WT (Fig 6C). We observed that the partially functional DdcA-GFP fusion was also present diffusely throughout the cytosol (Fig S3A). Finally, we tested DdcA localization using subcellular fractionation. We found that GFP-DdcA was detectable in the membrane and cytosolic fractions (Fig 6D), and similar results were obtained with DdcA-GFP (Fig S4B). As controls, we found that DdcP was found in the membrane fraction and not the cytosolic fraction (Fig 6D), and a cross-reacting protein detected by our GFP antiserum was found in the cytosol and not the membrane fractions (Fig 6D). Taken together, DdcA appears to be an intracellular protein that is primarily located in the cytosol with some molecules localized to the membrane. Thus, DdcA and the checkpoint recovery proteases are separated in space by the plasma membrane, which could partially explain why these factors have distinct functions.

DdcA inhibits YneA activity

DdcA appears to regulate YneA activity via a protease independent mechanism. We initially hypothesized that DdcA could interact with YneA to inhibit its activity. To test this hypothesis, we assayed for a protein-protein interaction using a bacterial two-hybrid, but did not detect an interaction (Fig S5). We then asked whether DdcA affected the localization of YneA. To address this question, we built a strain in which GFP was fused to the N-terminus of YneA, and placed *gfp-yneA* under the control of the xylose-inducible promoter P_{xyl}. We expressed both YneA and GFP-YneA in strains lacking *ddcA*, the checkpoint recovery proteases, or the triple mutant and found that GFP-YneA is able to inhibit growth to a similar extent as YneA (Fig 7A), suggesting that the GFP fusion is functional. We visualized GFP-YneA following induction with 0.1% xylose for 30 minutes. We found that GFP-YneA localized to the mid-cell, while also

demonstrating diffuse intracellular fluorescence (Fig 7B), which we suggest is free GFP generated by the checkpoint recovery proteases after YneA cleavage. Deletion of *ddcA* alone did not affect GFP-YneA localization, with both WT and Δ*ddcA* strains having similar mid-cell localization frequencies (Fig 7B). The absence of both checkpoint recovery proteases resulted in puncta throughout the plasma membrane (Fig 7B). Intriguingly, deletion of *ddcA* in addition to the checkpoint recovery proteases resulted in severe cell elongation, however, GFP-YneA localization was not affected (Fig 7B). The difference in cell length was quantified by measuring the cell length of at least 600 cells following growth in the presence of 0.1% xylose for 30 minutes. The cell length distributions of strains lacking *ddcA* or *ddcP* and *ctpA* were no different from the WT control (Fig 7C). The distribution for the strain lacking *ddcA*, *ddcP*, and *ctpA* had a significant skew to the right indicating greater cell lengths (Fig 7C). The percentage of cells greater than 5 μm in length was approximately 22% for the triple mutant and significantly greater than the other three strains in which approximately 1% of cells were greater than 5 μm (Table 1). As a control, we determined the cell length distributions prior to xylose addition and found all four strains to have similar cell length distributions in the absence of xylose (Fig 7C). We conclude that DdcA inhibits the activity of YneA without affecting its localization.

Discussion

A model for DNA damage checkpoint activation and recovery

The DNA damage checkpoint in bacteria was discovered through seminal work using *E. coli* as a model organism [7]. An underlying assumption in the models is that the input signal of RecA coated ssDNA and the affinity of LexA for its binding site is sufficient to control the rate of cell division in response to DNA damage. A finding that the initiator protein, DnaA, controls the

transcription of *ftsL*, and as a result the rate of cell division, in response to replication stress, gave a hint that coordination of cell division and DNA replication may be more complex [39]. Here, we elaborate on the complexity of regulating cell division in response to DNA damage by uncovering a DNA damage checkpoint antagonist, DdcA (Fig 8). In response to DNA damage, the repressor LexA is inactivated, which results in expression of *yneA*. Accumulation of YneA must saturate two proteases, DdcP and CtpA, and overcome DdcA-dependent inhibition in order to block cell division. After DNA repair occurs and the integrity of the DNA is restored the SOS response is terminated, LexA represses *yneA* expression and the checkpoint recovery proteases degrade the remaining YneA. Together, our results uncover a unique strategy in regulating a DNA damage checkpoint in bacteria.

How does DdcA inhibit YneA activity?

Our results are most supportive of DdcA acting as an antagonist to YneA, rather than functioning in checkpoint recovery. Two lines of evidence support this model. First, DdcA does not affect YneA protein levels or stability (Figs S3 & 4). Second, if DdcA was involved in checkpoint recovery, we would predict that expression of one of the checkpoint proteases would be able to compensate for deletion of *ddcA*. Instead, we found that the checkpoint recovery proteases and DdcA cannot replace each other (Fig 3). As a result, we hypothesize that DdcA acts by preventing YneA from accessing its target. We tested for an interaction between YneA and DdcA using a bacterial two-hybrid assay and we were unable to identify an interaction with full length or a cytoplasmic "locked" YneA mutant lacking its transmembrane domain (Fig S5). We also ruled out the hypothesis that DdcA affects the subcellular localization of YneA using a GFP-YneA fusion, which had similar localization patterns with and without *ddcA* (Fig 7B).

Taken together, all these results support a model where DdcA functions downstream of YneA by preventing access to the target of YneA.

The YneA target that results in the inhibition of cell division is unknown. YneA is a membrane bound cell division inhibitor. This class of inhibitor in bacteria is typified as being a small protein that contains an N-terminal transmembrane domain, and they have been identified in several species [21, 28-31, 56]. In *Caulobacter crescentus*, the cell division inhibitors SidA and DidA inhibit the activity of FtsW/N, which are components of the divisome [30, 31]. A recent study in *Staphylococcus aureus* identified a small membrane division inhibitor, SosA, and its target appears to be PBP1 [56], which is involved in peptidoglycan synthesis at the septum [57, 58]. It is tempting to speculate that YneA could target an essential component of the cell division machinery, because previous work found a conserved face of the transmembrane domain that is required for activity [22]. Still, there are fundamental differences between YneA and other membrane bound cell division inhibitors. YneA has two major predicted features: an N-terminal transmembrane domain and a C-terminal LysM domain, and both have been found to be required for full activity [22]. The other cell division inhibitors SidA, DidA, and SosA do not have a LysM domain [30, 31, 56]. LysM domains bind to the peptidoglycan (PG) cell wall and many proteins containing LysM domains have cell wall hydrolase activity [59]. Thus, another possibility is that the YneA acts directly on the cell wall to inhibit cell division. Intriguingly, the cell division inhibitor of *Mycobacterium tuberculosis*, Rv2719c, also contains a LysM domain and was shown to have cell wall hydrolase activity *in vitro* [28]. The localization of GFP-YneA is also similar to previous reports of fluorescent vancomycin labeling of nascent peptidoglycan synthesis [Fig 7B; 60, 61]. The difficulty with the model of targeting cell wall synthesis directly is that it is not clear how DdcA would prevent YneA activity given that these proteins are

348 separated by the plasma membrane. One explanation is that DdcA directly or indirectly affects
349 the folding of YneA as it is transported across the membrane, resulting in a form of YneA that is
350 not competent for PG binding. DdcA contains a TPR domain and proteins containing TPR
351 domains have been found to have chaperone activity and act as co-chaperones [62]. It is
352 intriguing that *ddcA* is just upstream of trigger factor (*tig*) in the *B. subtilis* genome, and this
353 organization is conserved in some bacterial species. In any case, to fully understand the function
354 of DdcA, the target of YneA would need to be elucidated first.

355 **Negative regulation of YneA occurs through three distinct mechanisms**

356 The checkpoint recovery proteases and DdcA utilize multiple strategies to inhibit YneA.
357 Although both DdcP and CtpA degrade YneA, they are very different proteases. DdcP has a Lon
358 peptidase domain and a PDZ domain, whereas CtpA has an S41 peptidase domain and a PDZ
359 domain. Intriguingly, the PDZ domains of DdcP and CtpA have different functions *in vivo* and
360 show homology to different classes of PDZ domains found in proteases in *E. coli* (FigS6, see
361 supplemental results). Thus, it appears that the proteases utilize different strategies to degrade
362 YneA. DdcA is unique, because it acts as an antagonist without affecting protein abundance,
363 stability, or localization. Also, DdcA appears to function prior to checkpoint establishment and
364 not in recovery, whereas the proteases perform both functions. Together, DdcA, DdcP, and CtpA
365 likely provide a buffer to expression of YneA, thereby setting a threshold of YneA for
366 checkpoint enforcement.

367 The discovery of a specific DNA damage checkpoint antagonist brings the total known
368 proteins to negatively regulate YneA to three, which begs the question: why isn't a single
369 protease sufficient? One explanation is that the process can be fine-tuned. By utilizing several

proteins, the process has more nodes for regulation, which is advantageous at least for *B. subtilis*. A second explanation is that this strategy evolved in response to more efficient DNA repair. The SOS-regulon is highly conserved in bacteria and yet the checkpoint strategies vary significantly [23]. If an organism evolves a more efficient DNA repair system, the same level of checkpoint protein will no longer be required. This could be the explanation for the highly divergent nature of cell division inhibitors in bacteria as well as the explanation for the complex control over YneA found in *B. subtilis*.

Materials and Methods

Bacteriological and molecular methods

All *B. subtilis* strains are derivatives of PY79 [63], and are listed in Table 2. Construction of individual strains is detailed in the supplemental methods using double cross-over recombination or CRISPR/Cas9 genome editing as previously described [38, 64]. *B. subtilis* strains were grown in LB (10 g/L NaCl, 10 g/L tryptone, 5 g/L yeast extract) or $S7_{50}$ media [1x $S7_{50}$ salts (diluted from 10x $S7_{50}$ salts: 104.7g/L MOPS, 13.2 g/L, ammonium sulfate, 6.8 g/L monobasic potassium phosphate, pH 7.0 adjusted with potassium hydroxide), 1x metals (diluted from 100x metals: 0.2 M $MgCl_2$, 70 mM $CaCl_2$, 5 mM $MnCl_2$, 0.1 mM $ZnCl_2$, 100 µg/mL thiamine-HCl, 2 mM HCl, 0.5 mM $FeCl_3$), 0.1% potassium glutamate, 40 µg/mL phenylalanine, 40 µg/mL tryptophan] containing either 2% glucose or 1% arabinose as indicated in each method. Plasmids used in this study are listed in Table S1. Individual plasmids were constructed using Gibson assembly as described previously [38, 65]. The details of plasmid construction are described in the supplemental methods. Oligonucleotides used in this study are listed in Table S2 and were obtained from Integrated DNA technologies (IDT). Antibiotics for selection in *B. subtilis* were

used at the following concentrations: 100 μg/mL spectinomycin, 5 μg/mL chloramphenicol, and 0.5 μg/mL erythromycin. Antibiotics used for selection in *Escherichia coli* were used at the following concentrations: 100 μg/mL spectinomycin, 100 μg/mL ampicillin, and 50 μg/mL kanamycin. Mitomycin C (Fisher bioreagents) and phleomycin (Sigma) were used at the concentrations indicated in the figures and legends.

Spot titer assays

Spot titer assays were performed as previously described [38]. Briefly, *B. subtilis* strains were grown on an LB agar plate at 30°C overnight and a single colony was used to inoculate a liquid LB culture. The cultures were grown at 37°C to an OD_{600} between 0.5 and 1. Cultures were normalized to an OD_{600} = 0.5, and serial dilutions were spotted on to LB agar media containing the drugs as indicated in the figures. Plates were grown at 30°C overnight (16-20 hours). All spot titer assays were performed at least twice.

Western blotting

Western blotting experiments for YneA were performed essentially as described [38]. Briefly, for the MMC recovery assay, samples of an OD_{600} = 10 were harvested via centrifugation and washed twice with 1x PBS pH 7.4 and re-suspended in 400 μL of sonication buffer (50 mM Tris, pH 8.0, 10 mM EDTA, 20% glycerol, 2x Roche protease inhibitors, and 5 mM PMSF) and lysed via sonication. SDS sample buffer was added to 2x and samples (10 μL) were incubated at 100°C and separated using 10% SDS-PAGE (DnaN) or 16.5% Tris-Tricine SDS-PAGE (YneA). Proteins were transferred to a nitrocellulose membrane using the BioRad transblot-turbo following the manufacturer's instructions. Membranes were blocked in 5% milk in TBST for 1 hour at room temperature. Membranes were incubated with YneA antiserum at a 1:3000 dilution

414 in 2% milk in TBST for two hours at room temperature or at 4°C overnight. Membranes were
415 washed three times with TBST for five minutes each and secondary antibodies (LiCor goat anti-
416 Rabbit-680LT; 1:15000) were added and incubated for one hour at room temperature.
417 Membranes were washed three times with TBST for five minutes each. Images of membranes
418 were captured using the LiCor Odyssey.

419 For overexpression of YneA, cultures of LB were inoculated at an OD_{600} = 0.05 and
420 incubated at 30°C until an OD_{600} of about 0.2 (about 90 minutes). Xylose was added to 0.1% and
421 cultures were incubated at 30°C for 2 hours. Samples of an OD_{600} = 25 were harvested and re-
422 suspended in 500 µL sonication buffer as above. All subsequent steps were performed as
423 described above.

424 For GFP-DdcA and DdcA-GFP, samples of an OD_{600} = 1 were harvested from LB +
425 0.05% xylose cultures via centrifugation and washed twice with 1x PBS pH 7.4. Samples were
426 re-suspended in 100 µL 1x SMM buffer (0.5 M sucrose, 0.02 M maleic acid, 0.02 M $MgCl_2$,
427 adjusted to pH 6.5) containing 1 mg/mL lysozyme and 2x Roche protease inhibitors. Samples
428 were incubated at room temperature for one hour and SDS sample buffer was added to 1x and
429 incubated at 100°C for 7 minutes. Samples (10 µL) were separated via 10% or 4-20% SDS-
430 PAGE. All subsequent steps were as described above, except GFP antisera (lot 1360-ex) was
431 used at a 1:5000 dilution at 4°C overnight.

432 **YneA stability assay**

433 Cultures of LB were inoculated at an OD_{600} = 0.05 and incubated at 30°C until an OD_{600} of about
434 0.2 (about 90 minutes). Xylose was added to 0.1% and cultures were incubated at 30°C for 2
435 hours. To stop translation, erythromycin was added to 50 µg/mL and samples (OD_{600} = 10) were

436 taken at 0, 60, 120, and 180 minutes (the strains for this experiment contain the chloramphenicol
437 resistant gene, *cat*, which prevents chloramphenicol from being used). Western blotting was
438 performed as described above.

439 **Subcellular fractionation**

440 Fractionation experiments were performed as described previously [48]. A cell pellet equivalent
441 to 1 mL OD_{600} = 1 was harvested via centrifugation (10,000 *g* for 5 minutes at room
442 temperature), and washed with 250 µL 1x PBS. Protoplasts were generated by resuspension in
443 100 µL 1x SMM buffer (0.5 M sucrose, 0.02 M maleic acid, 0.02 M $MgCl_2$, adjusted to pH 6.5)
444 containing 1 mg/mL lysozyme and 1x Roche protease inhibitors at room temperature for 2 hours.
445 Protoplasts were pelleted via centrifugation: 5,000 *g* for 6 minutes at room temperature.
446 Protoplasts were re-suspended in 100 µL TM buffer (20 mM Tris, pH 8.0, 5 mM $MgCl_2$, 40
447 units/mL DNase I (NEB), 200 µg/mL RNase A (Sigma), 0.5 mM $CaCl_2$, and 1x Roche protease
448 inhibitors) and left at room temperature for 30 minutes. The membrane fraction was pelleted via
449 centrifugation: 20,800 *g* for 30 minutes at 4°C. The cytosolic fraction (supernatant) was
450 transferred to a new tube and placed on ice, and the pellet was washed with 100 µL of TM buffer
451 and pelleted via centrifugation as above. The supernatant was discarded and the pellet was re-
452 suspended in 120 µL of 1x SDS dye. SDS loading dye was added to 1x to the cytosolic fraction
453 and 12 µL of each fraction were used for Western blot analysis.

454 **Culture supernatant protein precipitation**

455 Culture supernatants were concentrated by TCA precipitation as described previously with minor
456 modifications [66]. A culture was grown at 30°C until OD_{600} about 1, and the cells were pelleted
457 via centrifugation: 7,000 *g* for 10 minutes at room temperature. The culture supernatant (30 mL)

458 was filtered using a 0.22 μm filter and placed on ice. Proteins were precipitated by addition of 6
459 mL ice-cold 100% TCA (6.1N), and left on ice for 30 minutes. Precipitated proteins were
460 pelleted via centrifugation: 18,000 rpm (Sorvall SS-34 rotor) for 30 minutes at 4°C. Pellets were
461 washed with 1 mL ice-cold acetone and pelleted again via centrifugation: 20,000 *g* for 15
462 minutes at 4°C. The supernatant was discarded, and the residual acetone was evaporated by
463 placing tubes in 100°C heat block for 1-2 minutes. Protein pellets were re-suspended in 120 μL
464 6x SDS-loading dye and 12 μL were used in Western blot analysis.

465 **Proteinase K sensitivity assay**

466 Proteinase K sensitivity assays were performed similar to previous reports [49, 67]. A cell pellet
467 from 0.5 mL OD_{600} = 1 equivalent was harvested and washed as in "subcellular fractionation."
468 Protoplasts were generated by resuspension in 36 μL 1x SMM buffer (0.5 M sucrose, 0.02 M
469 maleic acid, 0.02 M $MgCl_2$, adjusted to pH 6.5) containing 1 mg/mL lysozyme at room
470 temperature for 1 hour. Either 9 μL of 1x SMM buffer or 0.5 mg/mL proteinase K (dissolved in
471 1x SMM buffer) was added (final proteinase K concentration of 100 μg/mL) and incubated at
472 37°C for the time indicated in the figures. Reactions were stopped by the addition of 5 μL 50
473 mM PMSF (final concentration of 5 mM) and 25 μL 6x SDS-dye (final concentration of 2x). For
474 Western blot analysis, 12 μL were used.

475 **Microscopy**

476 Strains were grown on LB agar plates containing 5 μg/mL chloramphenicol at 30°C overnight.
477 For GFP-DdcA and DdcA-GFP, LB agar plates were washed with $S7_{50}$ media containing 1%
478 arabinose and cultures of $S7_{50}$ media containing 1% arabinose and 0.05% xylose were inoculated
479 at an OD_{600} = 0.1 and incubated at 30°C until an OD_{600} of about 0.4. Samples were taken and

480 incubated with 2 µg/mL FM4-64 for 5 minutes and transferred to pads of 1x Spizizen salts and
481 1% agarose. Images were captured with an Olympus BX61 microscope using 250 ms and 1000
482 ms exposure times for FM4-64 (membranes) and GFP, respectively. The brightness and contrast
483 were adjusted for FM4-64 images with adjustments applied to the entire image. Strains with
484 GFP-YneA were grown on LB agar plates containing 5 µg/mL chloramphenicol overnight at
485 30°C. Plates were washed with $S7_{50}$ minimal media containing 1% arabinose and cultures started
486 at an OD_{600} = 0.1. Cultures were grown at 30°C until an OD_{600} of about 0.3 and xylose was
487 added to 0.1%. Cultures were grown for 30 minutes at 30°C and imaged as for GFP-DdcA with
488 exposure times of 300 ms for FM4-64 and 500 ms for GFP.

489 **Author contributions**

490 The study was conceived and designed by P.E.B. and L.A.S. Experiments were performed by
491 P.E.B. and Z.W.S. Data analysis was performed by P.E.B., Z.W.S., and L.A.S. The manuscript
492 was written and revised by P.E.B. and L.A.S.

493 **References**

494 1. Westfall CS, Levin PA. Bacterial Cell Size: Multifactorial and Multifaceted. Annual
495 review of microbiology. 2017;71:499-517. Epub 2017/09/10. doi: 10.1146/annurev-micro-
496 090816-093803. PubMed PMID: 28886685; PubMed Central PMCID: PMCPMC6018054.
497 2. Wang JD, Levin PA. Metabolism, cell growth and the bacterial cell cycle. Nature reviews
498 Microbiology. 2009;7(11):822-7. Epub 2009/10/07. doi: 10.1038/nrmicro2202. PubMed PMID:
499 19806155; PubMed Central PMCID: PMCPMC2887316.
500 3. Donachie WD, Blakely GW. Coupling the initiation of chromosome replication to cell
501 size in Escherichia coli. Current opinion in microbiology. 2003;6(2):146-50. Epub 2003/05/07.
502 PubMed PMID: 12732304.
503 4. Hill NS, Kadoya R, Chattoraj DK, Levin PA. Cell size and the initiation of DNA
504 replication in bacteria. PLoS Genet. 2012;8(3):e1002549. Epub 2012/03/08. doi:
505 10.1371/journal.pgen.1002549. PubMed PMID: 22396664; PubMed Central PMCID:
506 PMCPMC3291569.
507 5. Kreuzer KN. DNA damage responses in prokaryotes: regulating gene expression,
508 modulating growth patterns, and manipulating replication forks. Cold Spring Harb Perspect Biol.

509 2013;5(11):a012674. Epub 2013/10/08. doi: 10.1101/cshperspect.a012674. PubMed PMID:
510 24097899; PubMed Central PMCID: PMCPMC3809575.
511 6. Lenhart JS, Schroeder JW, Walsh BW, Simmons LA. DNA repair and genome
512 maintenance in Bacillus subtilis. Microbiology and molecular biology reviews : MMBR.
513 2012;76(3):530-64. Epub 2012/08/31. doi: 10.1128/mmbr.05020-11. PubMed PMID: 22933559;
514 PubMed Central PMCID: PMCPmc3429619.
515 7. Friedberg EC, Walker GC, Siede W, Wood RD, Schultz RA, Ellenberger T. DNA Repair
516 and Mutagenesis. 2nd ed. Washington, D.C.: ASM Press; 2006.
517 8. Ivancic-Bace I, Vlasic I, Salaj-Smic E, Brcic-Kostic K. Genetic evidence for the
518 requirement of RecA loading activity in SOS induction after UV irradiation in Escherichia coli.
519 Journal of bacteriology. 2006;188(14):5024-32. Epub 2006/07/04. doi: 10.1128/jb.00130-06.
520 PubMed PMID: 16816175; PubMed Central PMCID: PMCPMC1539949.
521 9. Anderson DG, Kowalczykowski SC. The translocating RecBCD enzyme stimulates
522 recombination by directing RecA protein onto ssDNA in a chi-regulated manner. Cell.
523 1997;90(1):77-86. Epub 1997/07/11. PubMed PMID: 9230304.
524 10. Churchill JJ, Anderson DG, Kowalczykowski SC. The RecBC enzyme loads RecA
525 protein onto ssDNA asymmetrically and independently of chi, resulting in constitutive
526 recombination activation. Genes & development. 1999;13(7):901-11. Epub 1999/04/10. PubMed
527 PMID: 10197989; PubMed Central PMCID: PMCPMC316600.
528 11. Morimatsu K, Kowalczykowski SC. RecFOR proteins load RecA protein onto gapped
529 DNA to accelerate DNA strand exchange: a universal step of recombinational repair. Mol Cell.
530 2003;11(5):1337-47. Epub 2003/05/29. PubMed PMID: 12769856.
531 12. Ivancic-Bace I, Peharec P, Moslavac S, Skrobot N, Salaj-Smic E, Brcic-Kostic K.
532 RecFOR function is required for DNA repair and recombination in a RecA loading-deficient
533 recB mutant of Escherichia coli. Genetics. 2003;163(2):485-94. Epub 2003/03/06. PubMed
534 PMID: 12618388; PubMed Central PMCID: PMCPMC1462458.
535 13. Slilaty SN, Little JW. Lysine-156 and serine-119 are required for LexA repressor
536 cleavage: a possible mechanism. Proceedings of the National Academy of Sciences of the United
537 States of America. 1987;84(12):3987-91. Epub 1987/06/01. PubMed PMID: 3108885; PubMed
538 Central PMCID: PMCPMC305006.
539 14. Little JW, Mount DW, Yanisch-Perron CR. Purified lexA protein is a repressor of the
540 recA and lexA genes. Proceedings of the National Academy of Sciences of the United States of
541 America. 1981;78(7):4199-203. Epub 1981/07/01. PubMed PMID: 7027255; PubMed Central
542 PMCID: PMCPMC319756.
543 15. Lewis LK, Harlow GR, Gregg-Jolly LA, Mount DW. Identification of high affinity
544 binding sites for LexA which define new DNA damage-inducible genes in Escherichia coli. J
545 Mol Biol. 1994;241(4):507-23. Epub 1994/08/26. doi: 10.1006/jmbi.1994.1528. PubMed PMID:
546 8057377.
547 16. Little JW, Mount DW. The SOS regulatory system of Escherichia coli. Cell.
548 1982;29(1):11-22. Epub 1982/05/01. PubMed PMID: 7049397.
549 17. Au N, Kuester-Schoeck E, Mandava V, Bothwell LE, Canny SP, Chachu K, et al.
550 Genetic composition of the Bacillus subtilis SOS system. Journal of bacteriology.
551 2005;187(22):7655-66. doi: 10.1128/jb.187.22.7655-7666.2005. PubMed PMID:
552 WOS:000233400200013.
553 18. Goranov AI, Kuester-Schoeck E, Wang JD, Grossman AD. Characterization of the global
554 transcriptional responses to different types of DNA damage and disruption of replication in

555 Bacillus subtilis. Journal of bacteriology. 2006;188(15):5595-605. doi: 10.1128/jb.00342-06.
556 PubMed PMID: WOS:000239366400029.
557 19. Huisman O, D'Ari R. An inducible DNA replication-cell division coupling mechanism in
558 E. coli. Nature. 1981;290(5809):797-9. Epub 1981/04/30. PubMed PMID: 7012641.
559 20. Huisman O, D'Ari R, Gottesman S. Cell-division control in Escherichia coli: specific
560 induction of the SOS function SfiA protein is sufficient to block septation. Proceedings of the
561 National Academy of Sciences of the United States of America. 1984;81(14):4490-4. Epub
562 1984/07/01. PubMed PMID: 6087326; PubMed Central PMCID: PMCPMC345616.
563 21. Kawai Y, Moriya S, Ogasawara N. Identification of a protein, YneA, responsible for cell
564 division suppression during the SOS response in Bacillus subtilis. Molecular microbiology.
565 2003;47(4):1113-22. Epub 2003/02/13. PubMed PMID: 12581363.
566 22. Mo AH, Burkholder WF. YneA, an SOS-induced inhibitor of cell division in Bacillus
567 subtilis, is regulated posttranslationally and requires the transmembrane region for activity.
568 Journal of bacteriology. 2010;192(12):3159-73. Epub 2010/04/20. doi: 10.1128/jb.00027-10.
569 PubMed PMID: 20400548; PubMed Central PMCID: PMCPMC2901685.
570 23. Erill I, Campoy S, Barbe J. Aeons of distress: an evolutionary perspective on the bacterial
571 SOS response. FEMS microbiology reviews. 2007;31(6):637-56. Epub 2007/09/22. doi:
572 10.1111/j.1574-6976.2007.00082.x. PubMed PMID: 17883408.
573 24. Bi E, Lutkenhaus J. Cell division inhibitors SulA and MinCD prevent formation of the
574 FtsZ ring. Journal of bacteriology. 1993;175(4):1118-25. Epub 1993/02/01. PubMed PMID:
575 8432706; PubMed Central PMCID: PMCPMC193028.
576 25. Huang J, Cao C, Lutkenhaus J. Interaction between FtsZ and inhibitors of cell division.
577 Journal of bacteriology. 1996;178(17):5080-5. Epub 1996/09/01. PubMed PMID: 8752322;
578 PubMed Central PMCID: PMCPMC178301.
579 26. Mukherjee A, Cao C, Lutkenhaus J. Inhibition of FtsZ polymerization by SulA, an
580 inhibitor of septation in Escherichia coli. Proceedings of the National Academy of Sciences of
581 the United States of America. 1998;95(6):2885-90. Epub 1998/04/18. PubMed PMID: 9501185;
582 PubMed Central PMCID: PMCPMC19664.
583 27. Trusca D, Scott S, Thompson C, Bramhill D. Bacterial SOS checkpoint protein SulA
584 inhibits polymerization of purified FtsZ cell division protein. Journal of bacteriology.
585 1998;180(15):3946-53. Epub 1998/07/31. PubMed PMID: 9683493; PubMed Central PMCID:
586 PMCPMC107380.
587 28. Chauhan A, Lofton H, Maloney E, Moore J, Fol M, Madiraju MV, et al. Interference of
588 Mycobacterium tuberculosis cell division by Rv2719c, a cell wall hydrolase. Molecular
589 microbiology. 2006;62(1):132-47. Epub 2006/09/01. doi: 10.1111/j.1365-2958.2006.05333.x.
590 PubMed PMID: 16942606.
591 29. Ogino H, Teramoto H, Inui M, Yukawa H. DivS, a novel SOS-inducible cell-division
592 suppressor in Corynebacterium glutamicum. Molecular microbiology. 2008;67(3):597-608. Epub
593 2007/12/19. doi: 10.1111/j.1365-2958.2007.06069.x. PubMed PMID: 18086211.
594 30. Modell JW, Hopkins AC, Laub MT. A DNA damage checkpoint in Caulobacter
595 crescentus inhibits cell division through a direct interaction with FtsW. Genes & development.
596 2011;25(12):1328-43. Epub 2011/06/21. doi: 10.1101/gad.2038911. PubMed PMID: 21685367;
597 PubMed Central PMCID: PMCPMC3127433.
598 31. Modell JW, Kambara TK, Perchuk BS, Laub MT. A DNA damage-induced, SOS-
599 independent checkpoint regulates cell division in Caulobacter crescentus. PLoS biology.

2014;12(10):e1001977. Epub 2014/10/29. doi: 10.1371/journal.pbio.1001977. PubMed PMID: 25350732; PubMed Central PMCID: PMCPMC4211646.

32. Canceill D, Dervyn E, Huisman O. Proteolysis and modulation of the activity of the cell division inhibitor SulA in Escherichia coli lon mutants. Journal of bacteriology. 1990;172(12):7297-300. Epub 1990/12/01. PubMed PMID: 2254289; PubMed Central PMCID: PMCPMC210862.

33. Mizusawa S, Gottesman S. Protein degradation in Escherichia coli: the lon gene controls the stability of sulA protein. Proceedings of the National Academy of Sciences of the United States of America. 1983;80(2):358-62. Epub 1983/01/01. PubMed PMID: 6300834; PubMed Central PMCID: PMCPMC393376.

34. Sonezaki S, Ishii Y, Okita K, Sugino T, Kondo A, Kato Y. Overproduction and purification of SulA fusion protein in Escherichia coli and its degradation by Lon protease in vitro. Applied microbiology and biotechnology. 1995;43(2):304-9. Epub 1995/05/01. PubMed PMID: 7612249.

35. Wu WF, Zhou Y, Gottesman S. Redundant in vivo proteolytic activities of Escherichia coli Lon and the ClpYQ (HslUV) protease. Journal of bacteriology. 1999;181(12):3681-7. Epub 1999/06/15. PubMed PMID: 10368141; PubMed Central PMCID: PMCPMC93844.

36. Seong IS, Oh JY, Yoo SJ, Seol JH, Chung CH. ATP-dependent degradation of SulA, a cell division inhibitor, by the HslVU protease in Escherichia coli. FEBS letters. 1999;456(1):211-4. Epub 1999/08/19. PubMed PMID: 10452560.

37. Kanemori M, Yanagi H, Yura T. The ATP-dependent HslVU/ClpQY protease participates in turnover of cell division inhibitor SulA in Escherichia coli. Journal of bacteriology. 1999;181(12):3674-80. Epub 1999/06/15. PubMed PMID: 10368140; PubMed Central PMCID: PMCPMC93843.

38. Burby PE, Simmons ZW, Schroeder JW, Simmons LA. Discovery of a dual protease mechanism that promotes DNA damage checkpoint recovery. PLoS Genet. 2018;14(7):e1007512. Epub 2018/07/07. doi: 10.1371/journal.pgen.1007512. PubMed PMID: 29979679.

39. Goranov AI, Katz L, Breier AM, Burge CB, Grossman AD. A transcriptional response to replication status mediated by the conserved bacterial replication protein DnaA. Proceedings of the National Academy of Sciences of the United States of America. 2005;102(36):12932-7. Epub 2005/08/27. doi: 10.1073/pnas.0506174102. PubMed PMID: 16120674; PubMed Central PMCID: PMCPMC1200305.

40. Cerveny L, Straskova A, Dankova V, Hartlova A, Ceckova M, Staud F, et al. Tetratricopeptide repeat motifs in the world of bacterial pathogens: role in virulence mechanisms. Infection and immunity. 2013;81(3):629-35. Epub 2012/12/25. doi: 10.1128/iai.01035-12. PubMed PMID: 23264049; PubMed Central PMCID: PMCPMC3584863.

41. Noll DM, Mason TM, Miller PS. Formation and repair of interstrand cross-links in DNA. Chemical reviews. 2006;106(2):277-301. Epub 2006/02/09. doi: 10.1021/cr040478b. PubMed PMID: 16464006; PubMed Central PMCID: PMCPmc2505341.

42. Iyer VN, Szybalski W. A molecular mechanism of mitomycin action: Linking of complementary DNA strands. Proceedings of the National Academy of Sciences of the United States of America. 1963;50:355-62. Epub 1963/08/01. PubMed PMID: 14060656; PubMed Central PMCID: PMCPmc221180.

644 43. Reiter H, Milewskiy M, Kelley P. Mode of action of phleomycin on Bacillus subtilis.
645 Journal of bacteriology. 1972;111(2):586-92. Epub 1972/08/01. PubMed PMID: 4626504;
646 PubMed Central PMCID: PMCPMC251321.
647 44. Kross J, Henner WD, Hecht SM, Haseltine WA. Specificity of deoxyribonucleic acid
648 cleavage by bleomycin, phleomycin, and tallysomycin. Biochemistry. 1982;21(18):4310-8. Epub
649 1982/08/31. PubMed PMID: 6181807.
650 45. Sancar A. DNA excision repair. Annual review of biochemistry. 1996;65:43-81. Epub
651 1996/01/01. doi: 10.1146/annurev.bi.65.070196.000355. PubMed PMID: 8811174.
652 46. Krogh A, Larsson B, von Heijne G, Sonnhammer EL. Predicting transmembrane protein
653 topology with a hidden Markov model: application to complete genomes. J Mol Biol.
654 2001;305(3):567-80. Epub 2001/01/12. doi: 10.1006/jmbi.2000.4315. PubMed PMID:
655 11152613.
656 47. Tjalsma H, Bolhuis A, Jongbloed JD, Bron S, van Dijl JM. Signal peptide-dependent
657 protein transport in Bacillus subtilis: a genome-based survey of the secretome. Microbiology and
658 molecular biology reviews : MMBR. 2000;64(3):515-47. Epub 2000/09/07. PubMed PMID:
659 10974125; PubMed Central PMCID: PMCPMC99003.
660 48. Wu LJ, Errington J. Septal localization of the SpoIIIE chromosome partitioning protein in
661 Bacillus subtilis. The EMBO journal. 1997;16(8):2161-9. Epub 1997/04/15. doi:
662 10.1093/emboj/16.8.2161. PubMed PMID: 9155041; PubMed Central PMCID:
663 PMCPMC1169818.
664 49. Wilson MJ, Carlson PE, Janes BK, Hanna PC. Membrane topology of the Bacillus
665 anthracis GerH germinant receptor proteins. Journal of bacteriology. 2012;194(6):1369-77. Epub
666 2011/12/20. doi: 10.1128/jb.06538-11. PubMed PMID: 22178966; PubMed Central PMCID:
667 PMCPMC3294866.
668 50. Buttner K, Bernhardt J, Scharf C, Schmid R, Mader U, Eymann C, et al. A
669 comprehensive two-dimensional map of cytosolic proteins of Bacillus subtilis. Electrophoresis.
670 2001;22(14):2908-35. Epub 2001/09/22. doi: 10.1002/1522-2683(200108)22:14<2908::aid-
671 elps2908>3.0.co;2-m. PubMed PMID: 11565787.
672 51. Eymann C, Dreisbach A, Albrecht D, Bernhardt J, Becher D, Gentner S, et al. A
673 comprehensive proteome map of growing Bacillus subtilis cells. Proteomics. 2004;4(10):2849-
674 76. Epub 2004/09/21. doi: 10.1002/pmic.200400907. PubMed PMID: 15378759.
675 52. Hirose I, Sano K, Shioda I, Kumano M, Nakamura K, Yamane K. Proteome analysis of
676 Bacillus subtilis extracellular proteins: a two-dimensional protein electrophoretic study.
677 Microbiology (Reading, England). 2000;146 (Pt 1):65-75. Epub 2000/02/05. doi:
678 10.1099/00221287-146-1-65. PubMed PMID: 10658653.
679 53. TMBASE - A database of membrane spanning protein segments [Internet]. 1993.
680 54. Bendtsen JD, Kiemer L, Fausboll A, Brunak S. Non-classical protein secretion in
681 bacteria. BMC microbiology. 2005;5:58. Epub 2005/10/11. doi: 10.1186/1471-2180-5-58.
682 PubMed PMID: 16212653; PubMed Central PMCID: PMCPMC1266369.
683 55. Yu NY, Wagner JR, Laird MR, Melli G, Rey S, Lo R, et al. PSORTb 3.0: improved
684 protein subcellular localization prediction with refined localization subcategories and predictive
685 capabilities for all prokaryotes. Bioinformatics (Oxford, England). 2010;26(13):1608-15. Epub
686 2010/05/18. doi: 10.1093/bioinformatics/btq249. PubMed PMID: 20472543; PubMed Central
687 PMCID: PMCPMC2887053.

688 56. Bojer MS, Wacnik K, Kjelgaard P, Gallay C, Bottomley AL, Cohn MT, et al. SosA
689 inhibits cell division in Staphylococcus aureus in response to DNA damage. bioRxiv. 2018. doi:
690 10.1101/364299.
691 57. Scheffers DJ, Errington J. PBP1 is a component of the Bacillus subtilis cell division
692 machinery. Journal of bacteriology. 2004;186(15):5153-6. Epub 2004/07/21. doi:
693 10.1128/jb.186.15.5153-5156.2004. PubMed PMID: 15262952; PubMed Central PMCID:
694 PMCPMC451649.
695 58. Claessen D, Emmins R, Hamoen LW, Daniel RA, Errington J, Edwards DH. Control of
696 the cell elongation-division cycle by shuttling of PBP1 protein in Bacillus subtilis. Molecular
697 microbiology. 2008;68(4):1029-46. Epub 2008/03/28. doi: 10.1111/j.1365-2958.2008.06210.x.
698 PubMed PMID: 18363795.
699 59. Buist G, Steen A, Kok J, Kuipers OP. LysM, a widely distributed protein motif for
700 binding to (peptido)glycans. Molecular microbiology. 2008;68(4):838-47. Epub 2008/04/24. doi:
701 10.1111/j.1365-2958.2008.06211.x. PubMed PMID: 18430080.
702 60. Daniel RA, Errington J. Control of cell morphogenesis in bacteria: two distinct ways to
703 make a rod-shaped cell. Cell. 2003;113(6):767-76. Epub 2003/06/18. PubMed PMID: 12809607.
704 61. Tiyanont K, Doan T, Lazarus MB, Fang X, Rudner DZ, Walker S. Imaging
705 peptidoglycan biosynthesis in Bacillus subtilis with fluorescent antibiotics. Proceedings of the
706 National Academy of Sciences of the United States of America. 2006;103(29):11033-8. Epub
707 2006/07/13. doi: 10.1073/pnas.0600829103. PubMed PMID: 16832063; PubMed Central
708 PMCID: PMCPMC1544169.
709 62. Smith DF. Tetratricopeptide repeat cochaperones in steroid receptor complexes. Cell
710 stress & chaperones. 2004;9(2):109-21. Epub 2004/10/23. PubMed PMID: 15497498; PubMed
711 Central PMCID: PMCPMC1065291.
712 63. Youngman P, Perkins JB, Losick R. Construction of a cloning site near one end of
713 TN917 into which foreign DNA may be inserted without affecting transposition in Bacillus
714 subtilis or expression of the transposon-bourne ERM gene. Plasmid. 1984;12(1):1-9. doi:
715 10.1016/0147-619x(84)90061-1. PubMed PMID: WOS:A1984TH41600001.
716 64. Burby PE, Simmons LA. MutS2 Promotes Homologous Recombination in Bacillus
717 subtilis. Journal of bacteriology. 2017;199(2). Epub 2016/11/02. doi: 10.1128/jb.00682-16.
718 PubMed PMID: 27799325; PubMed Central PMCID: PMCPMC5198493.
719 65. Gibson DG. Enzymatic assembly of overlapping DNA fragments. In: Voigt C, editor.
720 Synthetic Biology, Pt B: Computer Aided Design and DNA Assembly. Methods in Enzymology.
721 498. San Diego: Elsevier Academic Press Inc; 2011. p. 349-61.
722 66. Link AJ, LaBaer J. Trichloroacetic acid (TCA) precipitation of proteins. Cold Spring
723 Harbor protocols. 2011;2011(8):993-4. Epub 2011/08/03. doi: 10.1101/pdb.prot5651. PubMed
724 PMID: 21807853.
725 67. Navarre WW, Schneewind O. Proteolytic cleavage and cell wall anchoring at the LPXTG
726 motif of surface proteins in gram-positive bacteria. Molecular microbiology. 1994;14(1):115-21.
727 Epub 1994/10/01. PubMed PMID: 7830549.

728

Tables

Table 1 Over-expression of GFP-YneA results in a significant increase in cells greater than 5 µm in length in cells lacking *ddcP*, *ctpA*, and *ddcA*. Data are from expression of GFP-YneA using 0.1% xylose for 30 minutes. The mean cell length ± the standard deviation is listed. The percent of cells greater than 5 µm (number/total cells scored), with the p-value from a two-tailed z-test are listed.

		No Xylose	0.1% Xylose		
Strain	**Genotype**	**Cell length (mean ± sd)**	**Cell length (mean ± sd)**	**% ≥ 5 µm**	**p-value**
PEB876	*amyE::P$_{xyl}$-gfp-yneA*	1.98 ± 0.51 (n = 685)	2.91 ± 0.75	0.84% (6/717)	N/A
PEB882	Δ*ddcA*, *amyE::P$_{xyl}$-gfp-yneA*	2.48 ± 0.73 (n = 672)	2.86 ± 0.85	1.16% (7/601)	0.55
PEB888	Δ*ddcP*, Δ*ctpA*, *amyE::P$_{xyl}$-gfp-yneA*	2.18 ± 0.60 (n = 690)	2.49 ± 0.70	0.68% (5/734)	0.73
PEB894	Δ*ddcP*, Δ*ctpA*, Δ*ddcA*, *amyE::P$_{xyl}$-gfp-yneA*	2.39 ± 1.10 (n = 695)	4.09 ± 2.09	22.4% (159/711)	>0.00001

Table 2 Strains used in this study

Strain	Genotype	Reference
PY79	PY79	[63]
PEB309	Δ*uvrAB*	This study
PEB324	Δ*ddcP* (*ylbL*)	[38]
PEB355	Δ*ctpA*	[38]
PEB357	Δ*ddcA* (*ysoA*)	[38]
PEB433	Δ*yneA::erm*	[38]
PEB439	Δ*yneA::loxP*	[38]
PEB495	Δ*ddcA*, Δ*yneA::erm*	This study
PEB497	Δ*uvrAB*, Δ*ddcA*	This study
PEB499	Δ*ddcP*, Δ*ddcA*	This study
PEB503	Δ*ddcA*, *amyE::P$_{xyl}$-ddcA*	This study
PEB555	Δ*ddcP*, Δ*ctpA*	[38]
PEB557	Δ*ddcP*, Δ*ctpA*, *amyE::P$_{xyl}$-ddcP*	[38]
PEB561	Δ*ddcP*, Δ*ctpA*, Δ*yneA::loxP*	[38]
PEB579	Δ*ctpA*, Δ*ddcA*	This study
PEB587	Δ*ddcA*, Δ*yneA::loxP*	This study
PEB619	Δ*ddcP*, Δ*ctpA*, *amyE::P$_{xyl}$-ctpA*	[38]
PEB639	Δ*ddcP*, Δ*ctpA*, Δ*ddcA*	This study
PEB643	Δ*ddcP*, Δ*ctpA*, Δ*ddcA*, Δ*yneA::loxP*	This study
PEB719	Δ*ddcP*, *amyE::P$_{xyl}$-ddcP*Δ*TM*	This study

PEB772	Δ*ctpA, amyE::P$_{xyl}$-ctpAΔTM*	This study
PEB774	*ddcPΔPDZ*	This study
PEB776	*ctpAΔPDZ*	This study
PEB836	Δ*ddcA*, *amyE::P$_{xyl}$-ddcP*	This study
PEB837	Δ*ddcA*, *amyE::P$_{xyl}$-ctpA*	This study
PEB838	Δ*ddcP,* Δ*ctpA*, *amyE::P$_{xyl}$-ddcA*	This study
PEB839	Δ*ddcP,* Δ*ctpA*, Δ*ddcA*, *amyE::P$_{xyl}$-ddcP*	This study
PEB840	Δ*ddcP,* Δ*ctpA*, Δ*ddcA*, *amyE::P$_{xyl}$-ddcA*	This study
PEB841	Δ*ddcP,* Δ*ctpA*, Δ*ddcA*, *amyE::P$_{xyl}$-ctpA*	This study
PEB846	*amyE::P$_{xyl}$-yneA*	This study
PEB848	Δ*ddcA*, *amyE::P$_{xyl}$-yneA*	This study
PEB850	Δ*ddcP,* Δ*ctpA*, *amyE::P$_{xyl}$-yneA*	This study
PEB852	Δ*ddcP,* Δ*ctpA*, Δ*ddcA*, *amyE::P$_{xyl}$-yneA*	This study
PEB854	Δ*ddcA*, *amyE::P$_{xyl}$-gfp-ddcA*	This study
PEB856	Δ*ddcA*, *amyE::P$_{xyl}$-ddcA-gfp*	This study
PEB876	*amyE::P$_{xyl}$-gfp-yneA*	This study
PEB882	Δ*ddcA*, *amyE::P$_{xyl}$-gfp-yneA*	This study
PEB888	Δ*ddcP,* Δ*ctpA*, *amyE::P$_{xyl}$-gfp-yneA*	This study
PEB894	Δ*ddcP,* Δ*ctpA*, Δ*ddcA*, *amyE::P$_{xyl}$-gfp-yneA*	This study

Figure Legends

Figure 1. Deletion of *ddcA* (*ysoA*) results in sensitivity to DNA damage. (A) A schematic of the DdcA protein. DdcA is predicted to have 334 amino acids and 3 tetratrichopeptide repeats at its N-terminus. **(B)** A spot titer assay in which exponentially growing cultures of *B. subtilis* strains WT (PY79), Δ*ddcA* (PEB357), and Δ*ddcA*, *amyE::P$_{xyl}$-ddcA* (PEB503) were spotted on the indicated media and incubated at 30°C overnight.

Figure 2. DdcA functions independent of the checkpoint recovery proteases. (A) Spot titer assay using *B. subtilis* strains WT (PY79), Δ*ddcA* (PEB357), Δ*ddcP* (PEB324), Δ*ddcA* Δ*ddcP* (PEB499), Δ*ctpA* (PEB355), and Δ*ddcA* Δ*ctpA* (PEB579) spotted on the indicated media. **(B)** Spot titer assay using *B. subtilis* strains WT (PY79), Δ*ddcA* (PEB357), Δ*ddcP* Δ*ctpA* (PEB555), Δ*ddcA* Δ*ddcP* Δ*ctpA* (PEB639), Δ*yneA::loxP* (PEB439), Δ*ddcA* Δ*yneA::loxP* (PEB587), Δ*ddcP*

Δ*ctpA* Δ*yneA::loxP* (PEB561), and Δ*ddcA* Δ*ddcP* Δ*ctpA* Δ*yneA::loxP* (PEB643) spotted on the indicated media.

Figure 3. DdcA cannot complement loss of checkpoint recovery proteases. (A) Spot titer assay using *B. subtilis* strains WT (PY79), Δ*ddcA* (PEB357), Δ*ddcA amyE::P_{xyl}-ddcP* (PEB836), and Δ*ddcA amyE::P_{xyl}-ctpA* (PEB837) spotted on the indicated media. **(B)** Spot titer assay using *B. subtilis* strains WT (PY79), Δ*ddcP* Δ*ctpA* (PEB555), Δ*ddcP,* Δ*ctpA*, *amyE::P_{xyl}-ddcA* (PEB838), Δ*ddcP,* Δ*ctpA*, *amyE::P_{xyl}-ddcP* (PEB557), Δ*ddcA* Δ*ddcP* Δ*ctpA* (PEB639), Δ*ddcP,* Δ*ctpA*, Δ*ddcA*, *amyE::P_{xyl}-ddcA* (PEB840), Δ*ddcP,* Δ*ctpA*, Δ*ddcA*, *amyE::P_{xyl}-ddcP* (PEB839), and Δ*ddcP,* Δ*ctpA*, Δ*ddcA*, *amyE::P_{xyl}-ctpA* (PEB841) spotted on the indicated media. **(C)** Spot titer assay using *B. subtilis* strains WT (PY79), Δ*ddcP* Δ*ctpA* (PEB555), Δ*ddcP,* Δ*ctpA*, *amyE::P_{xyl}-ddcA* (PEB838), Δ*ddcA* Δ*ddcP* Δ*ctpA* (PEB639), Δ*ddcP,* Δ*ctpA*, and Δ*ddcA*, *amyE::P_{xyl}-ddcA* (PEB840) spotted on the indicated media.

Figure 4. Deletion of *ddcA* results in sensitivity to *yneA* overexpression independent of YneA stability. (A) Spot titer testing the effect of *yneA* overexpression. *B. subtilis* strains WT (PY79), *amyE::P_{xyl}-yneA* (PEB846), Δ*ddcA amyE::P_{xyl}-yneA* (PEB848), Δ*ddcP,* Δ*ctpA*, *amyE::P_{xyl}-yneA* (PEB850), and Δ*ddcA* Δ*ddcP* Δ*ctpA, amyE::P_{xyl}-yneA* (PEB852) were spotted on LB agar media containing increasing concentrations of xylose to induce *yneA* expression. **(B)** A Western blot using antisera against YneA (Upper panels), or DnaN lower panel using *B. subtilis* strains WT (PY79), *amyE::P_{xyl}-yneA* (PEB846), Δ*ddcA amyE::P_{xyl}-yneA* (PEB848), Δ*ddcP,* Δ*ctpA*, *amyE::P_{xyl}-yneA* (PEB850), and Δ*ddcA* Δ*ddcP* Δ*ctpA, amyE::P_{xyl}-yneA* (PEB852) after growing in the presence of 0.1% xylose for two hours. The panel on the left shows an increased exposure to see the faint bands of WT and Δ*ddcA*. **(C)** A Western blot using antisera

771 against YneA (upper panel) or DnaN (lower panel). Cultures of Δ*ddcP,* Δ*ctpA*, *amyE::P*$_{xyl}$*-yneA*
772 (PEB850) and Δ*ddcA* Δ*ddcP* Δ*ctpA, amyE::P*$_{xyl}$*-yneA* (PEB852) were grown as in panel B,
773 except at 0 hours erythromycin was added and samples were harvest every hour for three hours.

774 **Figure 5. DdcP and CtpA are membrane anchored with extracellular protease domains (A)**
775 Subcellular fractionation followed by Western blot analysis of WT (PY79) lysates using DdcP
776 and CtpA antiserum (M, molecular weight standard, WCL, whole cell lysates; Media,
777 precipitated media proteins; Cyt, cytosolic fraction; Mem, membrane fraction). **(B)** Competing
778 models for membrane topology of DdcP and CtpA tested with proteinase K sensitivity assay. **(C)**
779 Proteinase K sensitivity assay followed by Western blot detection of DdcP, CtpA, and DnaN
780 with antiserum. Samples were treated with lysozyme to generate protoplasts and incubated with
781 proteinase K for the indicated time (lanes 1-6), or the samples were incubated with lysozyme and
782 Triton X-100 to disrupt the plasma membrane and incubated with proteinase K for the indicated
783 time (lanes 7-9). **(D)** Schematics depicting the DdcPΔTM (left) and CtpAΔTM (right) in which
784 the transmembrane domain was deleted. **(E)** Proteinase K sensitivity assay followed by Western
785 blot analysis of strains expressing DdcPΔTM (left, PEB719) or CtpAΔTM (right, PEB772)
786 performed as in panel C using a 2 hour incubation with proteinase K.

787 **Figure 6. GFP-DdcA is an intracellular protein and is present in the cytosolic and**
788 **membrane fractions. (A)** Spot titer assay using *B. subtilis* strains WT (PY79), Δ*ddcA*
789 (PEB357), Δ*ddcA amyE::P*$_{xyl}$*-gfp-ddcA* (PEB854), and Δ*ddcA amyE::P*$_{xyl}$*-ddcA-gfp* (PEB856)
790 spotted on the indicated media. **(B)** Western blot of cell extracts from *B. subtilis* strains WT
791 (PY79), Δ*ddcA amyE::P*$_{xyl}$*-gfp-ddcA* (PEB854), and Δ*ddcA amyE::P*$_{xyl}$*-ddcA-gfp* (PEB856) using
792 antiserum against GFP. The arrowhead highlights the slightly increased mobility of DdcA-GFP,
793 and the asterisk denotes a cross-reacting species detected by the GFP antiserum. The smaller

794 arrow indicates the expected migration of free GFP. **(C)** Micrographs from WT (PY79) and
795 Δ*ddcA amyE::P$_{xyl}$-gfp-ddcA* (PEB854) cultures grown in S7$_{50}$ minimal media containing 1%
796 arabinose with (far left and right panels) or without (middle panels) 0.05% xylose. Images in red
797 are the membrane stain FM4-64, green are GFP fluorescence and the bottom images are a merge
798 of FM4-64 and GFP fluorescence. The white lines through cells in the images are a
799 representation of the line scans of fluorescence intensity generated in ImageJ and plotted below
800 the micrographs. Scale bar is 5 μm. **(D)** Western blot of whole cell lysate (WCL), cytosolic
801 fraction (Cyt), and membrane fraction (Mem) from Δ*ddcA amyE::P$_{xyl}$-gfp-ddcA* (PEB854) cell
802 extracts using antisera against GFP (upper panel) or DdcP (lower panel). The asterisk denotes a
803 cross-reacting species detected by the GFP antiserum.

804 **Figure 7. DdcA inhibits YneA activity (A)** *B. subtilis* strains *amyE::P$_{xyl}$-yneA* (PEB846),
805 Δ*ddcA amyE::P$_{xyl}$-yneA* (PEB848), Δ*ddcP,* Δ*ctpA*, *amyE::P$_{xyl}$-yneA* (PEB850), and Δ*ddcA*
806 Δ*ddcP* Δ*ctpA, amyE::P$_{xyl}$-yneA* (PEB852), *amyE::P$_{xyl}$-gfp-yneA* (PEB876), Δ*ddcA amyE::P$_{xyl}$-*
807 *gfp-yneA* (PEB882), Δ*ddcP,* Δ*ctpA*, *amyE::P$_{xyl}$-gfp-yneA* (PEB888), and Δ*ddcA* Δ*ddcP* Δ*ctpA,*
808 *amyE::P$_{xyl}$-gfp-yneA* (PEB894) were struck onto LB or LB + 0.1% xylose and incubated at 30°C
809 overnight. **(B)** Micrographs from the indicated strains from Panel A, grown in minimal media
810 and treated with 0.1% xylose for 30 minutes. Green images are GFP fluorescence and red images
811 are FM4-64 membrane stain. The percentage of septal localization is shown for PEB876 (n=591)
812 and PEB882 (n=542). The p-value of a two-tailed z-test was 0.516. **(C)** Cell length distributions
813 of strains grown with (right) or without (left) 0.1% xylose. The number of cells measured (n) for
814 each condition is indicated.

815 **Figure 8. DdcA inhibits enforcement of the DNA damage checkpoint.** A working model for
816 how DdcA inhibits the activity of YneA. DdcA prevents access to the target of YneA, however,

817 when the SOS response has been activated for a prolonged period of time, YneA is able to
818 overcome DdcA dependent inhibition to prevent cell division. Following DNA repair and
819 completion of DNA replication the SOS response is turned off and the checkpoint recovery
820 proteases degrade YneA allowing cell division to resume.

821 **Supplemental Figure Legends**

822 **Figure S1 DNA damage sensitivity of *ddcA* deletion is dependent on DNA damage**
823 **checkpoint protein YneA and independent of nucleotide excision repair.** A spot titer assay
824 using *B. subtilis* strains WT (PY79), Δ*ddcA* (PEB357), Δ*uvrAB* (PEB309), Δ*yneA::erm*
825 (PEB433), Δ*ddcA* Δ*yneA::erm* (PEB495), and Δ*ddcA* Δ*uvrAB* (PEB497) spotted on the indicated
826 media.

827 **Figure S2 Deletion of *ddcA* can be complemented by ectopic expression using high levels of**
828 **xylose.** A Spot titer assay using WT (PY79), Δ*ddcA* (PEB357), and Δ*ddcA amyE::P_{xyl}-ddcA*
829 (PEB503) spotted on the indicated media and incubated at 30°C overnight.

830 **Figure S3 Deletion of *ddcA* does not increase YneA protein levels following MMC**
831 **treatment and recovery.** Western blotting using antisera against YneA (top panel) or DnaN
832 (bottom panel) using whole cell extracts from WT (PY79), Δ*ddcA* (PEB357), Δ*ddcP* Δ*ctpA*
833 (PEB555), Δ*ddcA* Δ*ddcP* Δ*ctpA* (PEB639) after a two hour treatment with 100 ng/mL MMC
834 (lanes labeled "MMC") or after recovering for two hours from MMC treatment (lanes labeled
835 "2h Rec").

836 **Figure S4 DdcA-GFP is intracellular and found in the cytosolic and membrane fractions.**
837 **(A)** Micrographs from WT (PY79) and Δ*ddcA amyE::P_{xyl}-ddcA-gfp* (PEB856) cultures grown in
838 $S7_{50}$ minimal media containing 1% arabinose and 0.05% xylose. Images in red are the membrane

839 stain FM4-64, green are GFP fluorescence and the bottom images are a merge of FM4-64 and
840 GFP fluorescence. The white lines through cells in the images are a representation of the line
841 scans of fluorescence intensity generated in ImageJ and plotted below the micrographs. Scale bar
842 is 5 μm. **(B)** Western blot of the whole cell lysate (WCL), cytosolic fraction (Cyt), and
843 membrane fraction (Mem) from Δ*ddcA amyE::*P_{xyl}*-ddcA-gfp* (PEB856) cell extracts using
844 antisera against GFP (upper panel) or DdcP (lower panel). The asterisk denotes a cross-reacting
845 species detected by the GFP antiserum.

846 **Figure S5 DdcA and YneA do not interact in bacterial two hybrid assay** Plasmids containing
847 the indicated T18 (rows) and T25 (columns) fusions were used to co-transform *E. coli* BTH101
848 cells, which were spotted onto LB containing X-gal and IPTG.

849 **Figure S6 DdcP and CtpA PDZ domains have different functions *in vivo* (A)** Alignment of
850 the PDZ domain of DdcP to the PDZ domains of DegP and DegS from *E. coli*. **(B)** Alignment of
851 the PDZ domain of CtpA to the PDZ domains of CtpB from *B. subtilis* and Prc from *E. coli*. **(C)**
852 Schematics of ΔPDZ constructs used in panels B and C. **(D)** Spot titer assay using *B. subtilis*
853 strains WT (PY79), Δ*ddcP* (PEB324), *ddcP*Δ*PDZ* (PEB774), Δ*ctpA* (PEB355), and *ctpA*Δ*PDZ*
854 (PEB776) media. **(E)** Western blot analysis of WT (PY79), *ddcP*Δ*PDZ* (PEB774), and
855 *ctpA*Δ*PDZ* (PEB776) cell lysates using DdcP, CtpA, and DnaN antiserum.

856 **Supplemental text containing supplemental tables, results, and methods.**

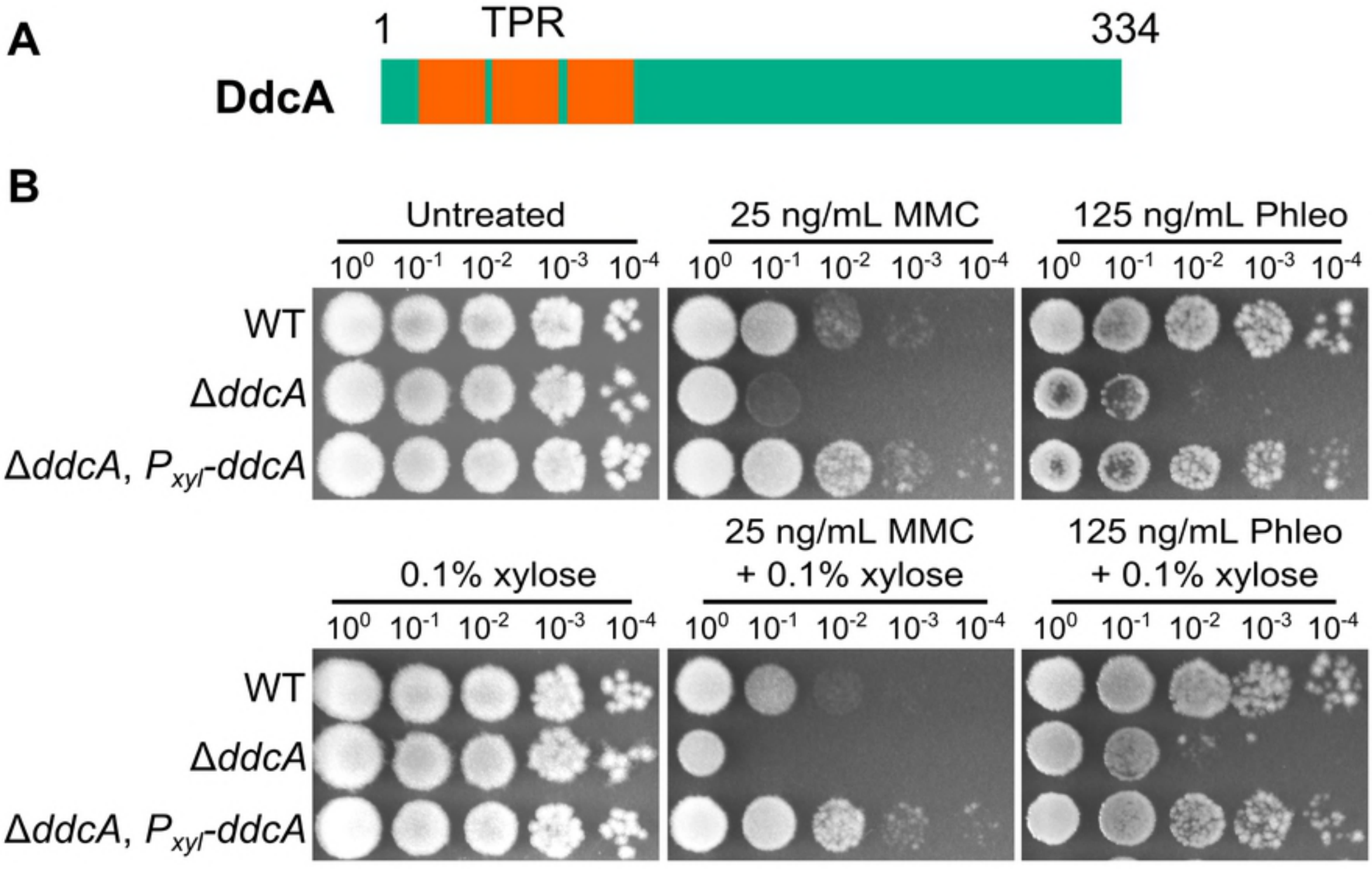
A
1
TPR
334
DdcA
B
Untreated
25 ng/mL MMC
125 ng/mL Phleo
10^0 10^-1 10^-2 10^-3 10^-4
WT
ΔddcA
ΔddcA, P_xyl-ddcA
0.1% xylose
25 ng/mL MMC
+ 0.1% xylose
125 ng/mL Phleo
+ 0.1% xylose

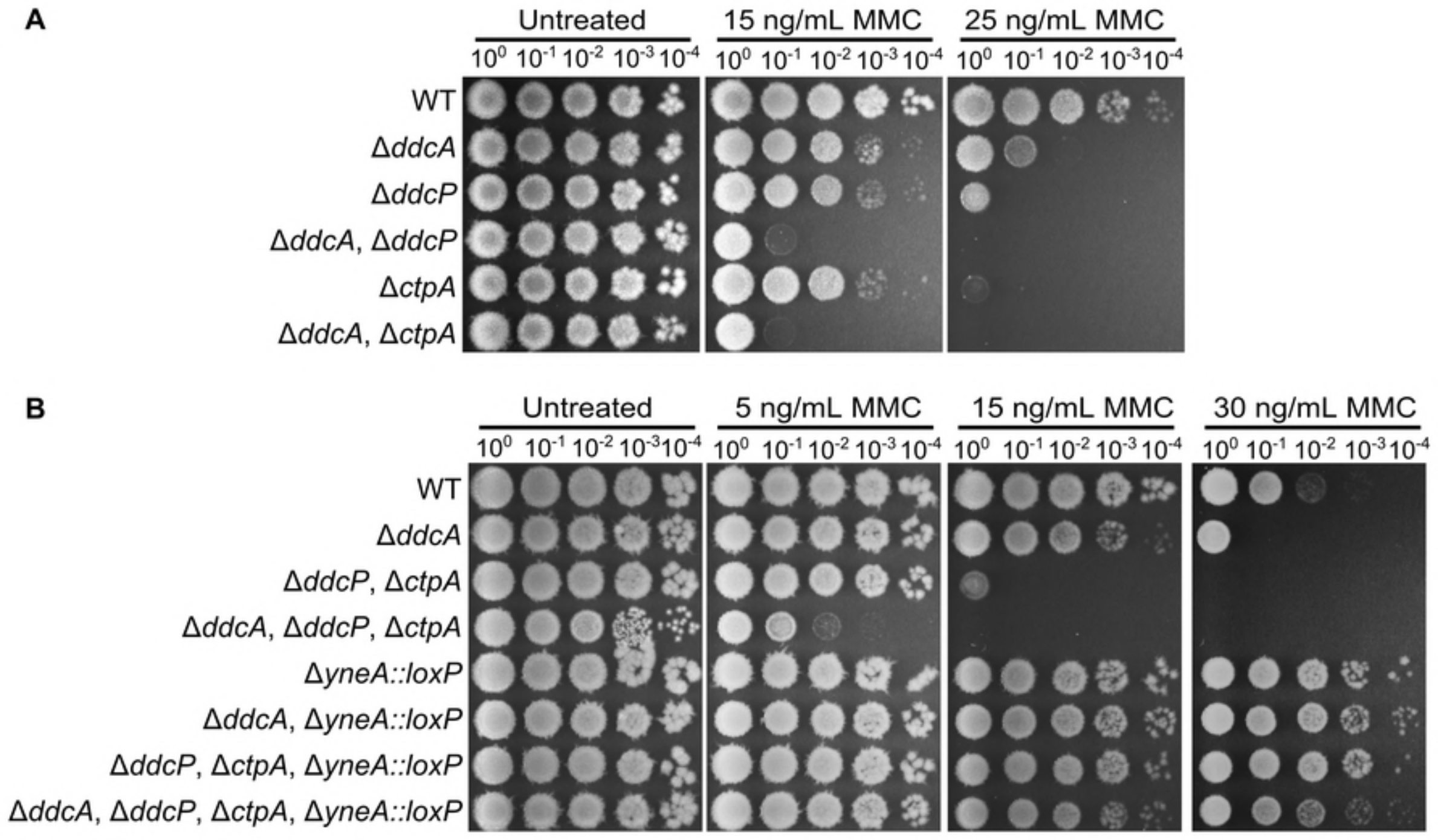
A
Untreated
15 ng/mL MMC
25 ng/mL MMC
10^0 10^-1 10^-2 10^-3 10^-4
WT
ΔddcA
ΔddcP
ΔddcA, ΔddcP
ΔctpA
ΔddcA, ΔctpA
B
Untreated
5 ng/mL MMC
15 ng/mL MMC
30 ng/mL MMC
10^0 10^-1 10^-2 10^-3 10^-4
WT
ΔddcA
ΔddcP, ΔctpA
ΔddcA, ΔddcP, ΔctpA
ΔyneA::loxP
ΔddcA, ΔyneA::loxP
ΔddcP, ΔctpA, ΔyneA::loxP
ΔddcA, ΔddcP, ΔctpA, ΔyneA::loxP

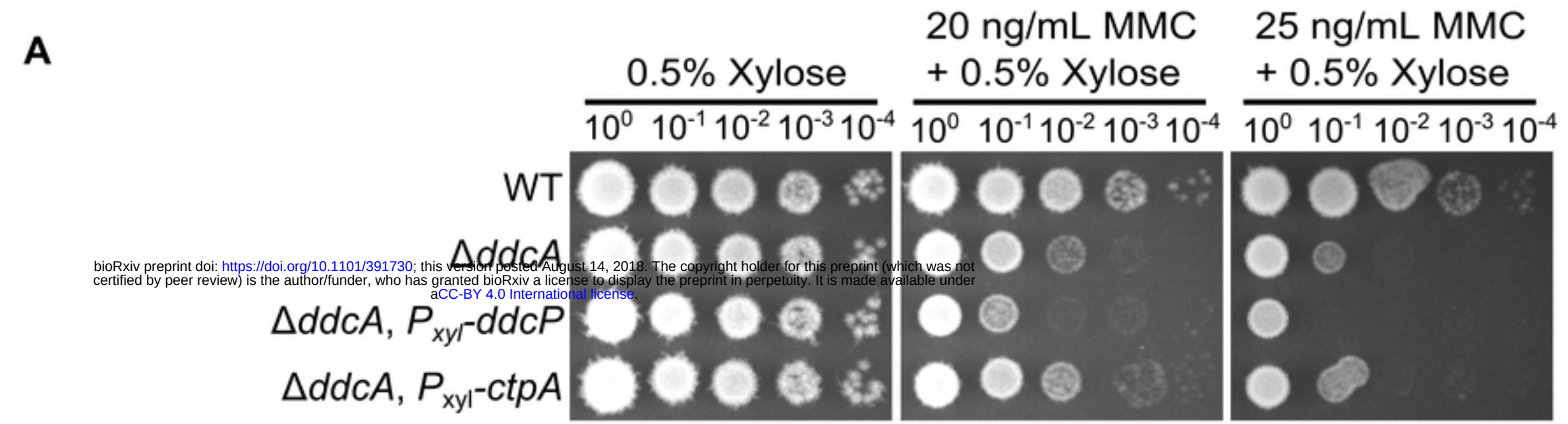

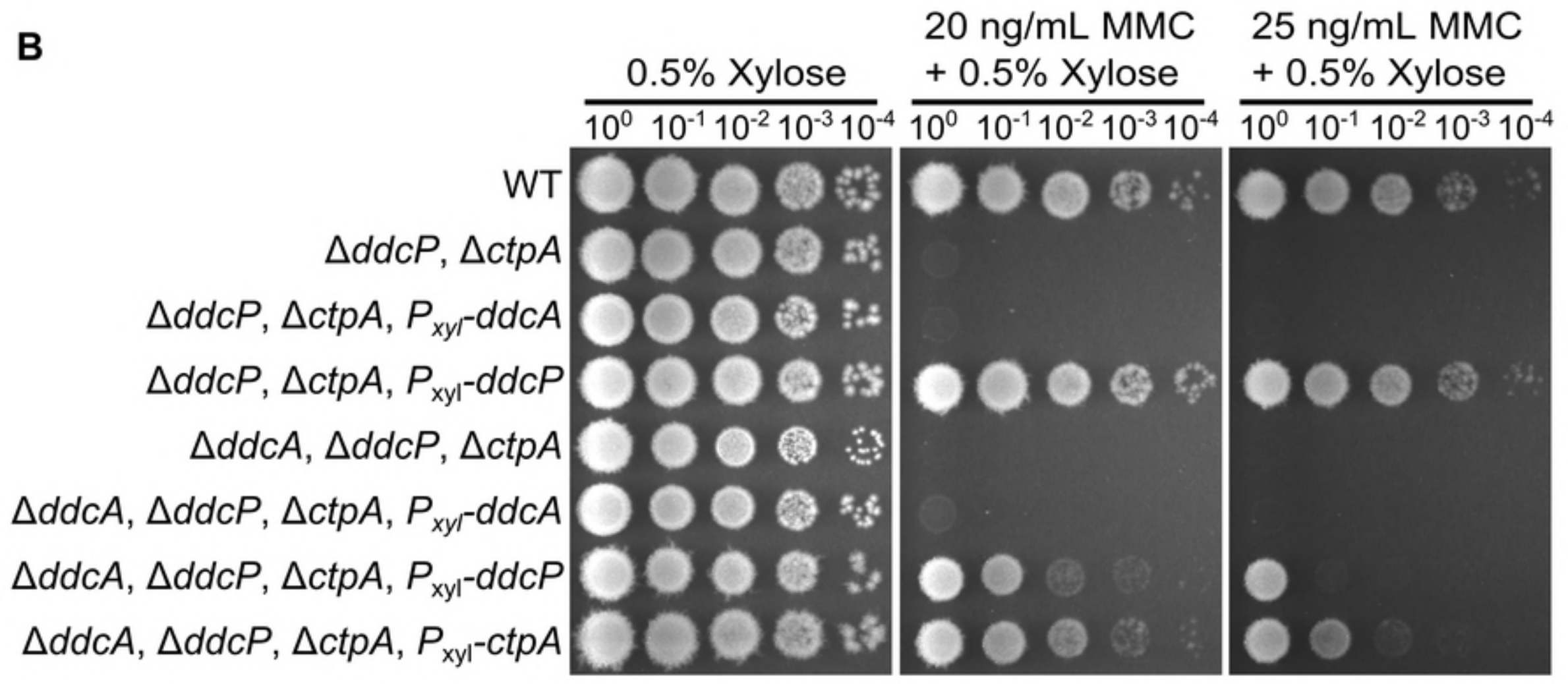

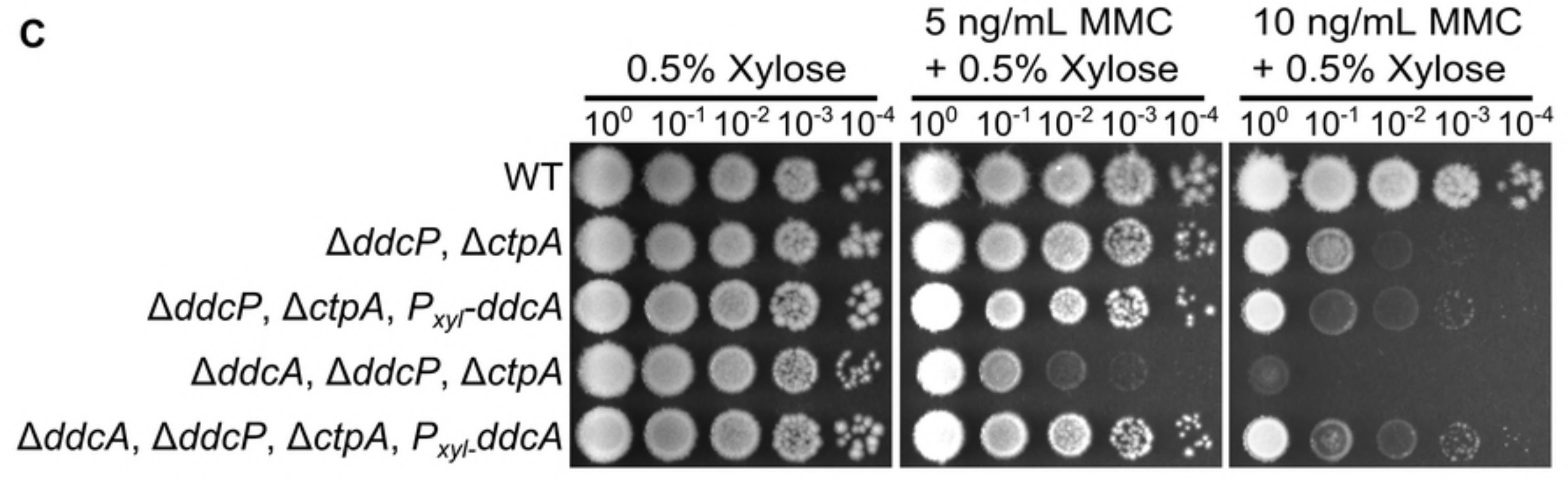

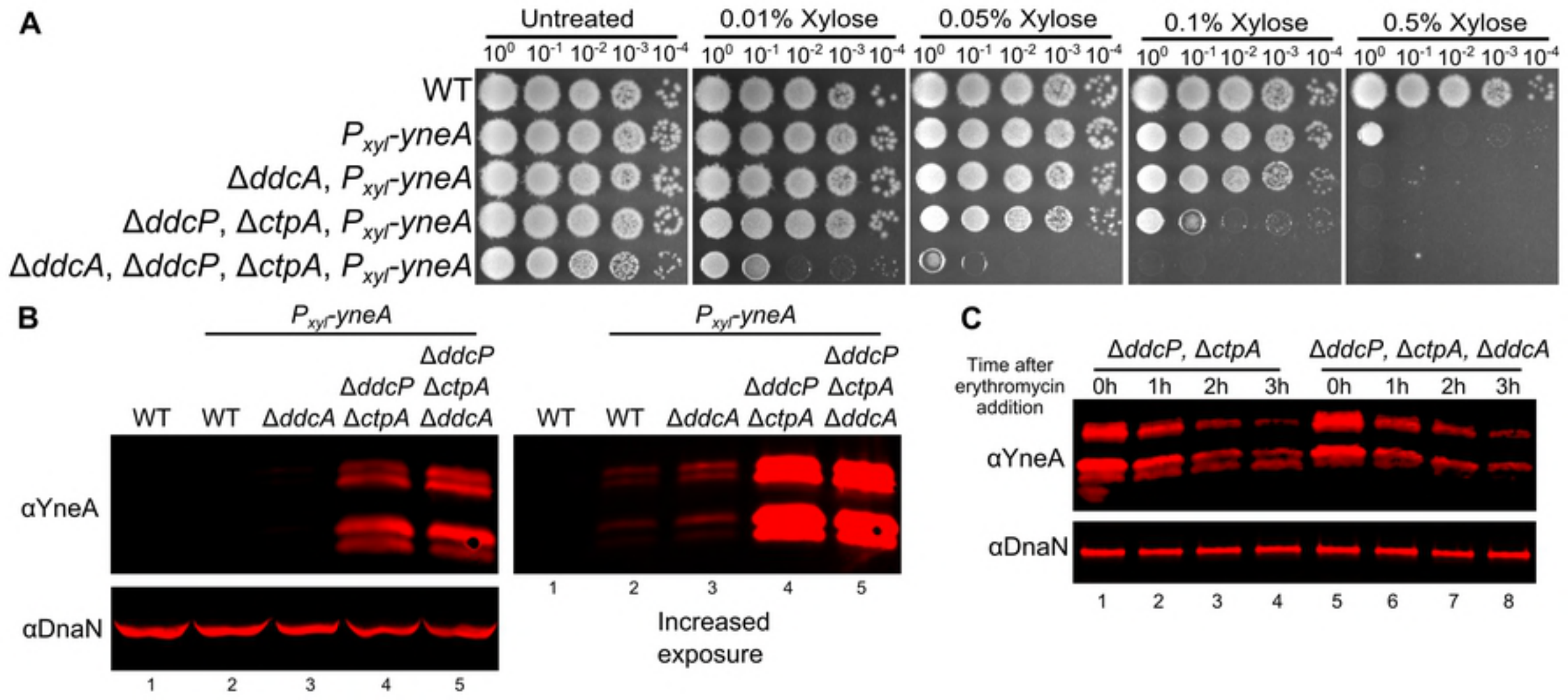
A
Untreated
0.01% Xylose
0.05% Xylose
0.1% Xylose
0.5% Xylose
10^0 10^-1 10^-2 10^-3 10^-4
WT
P_xyl-yneA
ΔddcA, P_xyl-yneA
ΔddcP, ΔctpA, P_xyl-yneA
ΔddcA, ΔddcP, ΔctpA, P_xyl-yneA
B
P_xyl-yneA
WT WT ΔddcA ΔddcP ΔctpA ΔddcP ΔctpA ΔddcA
αYneA
αDnaN
1 2 3 4 5
Increased exposure
C
Time after erythromycin addition
ΔddcP, ΔctpA
ΔddcP, ΔctpA, ΔddcA
0h 1h 2h 3h 0h 1h 2h 3h
αYneA
αDnaN
1 2 3 4 5 6 7 8

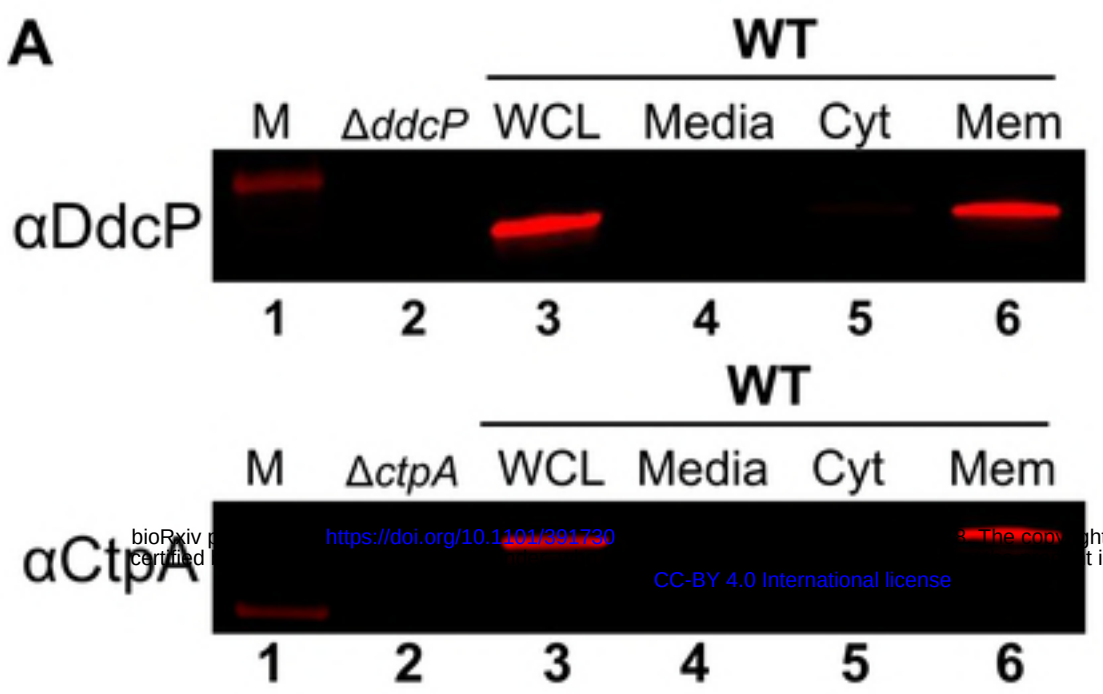

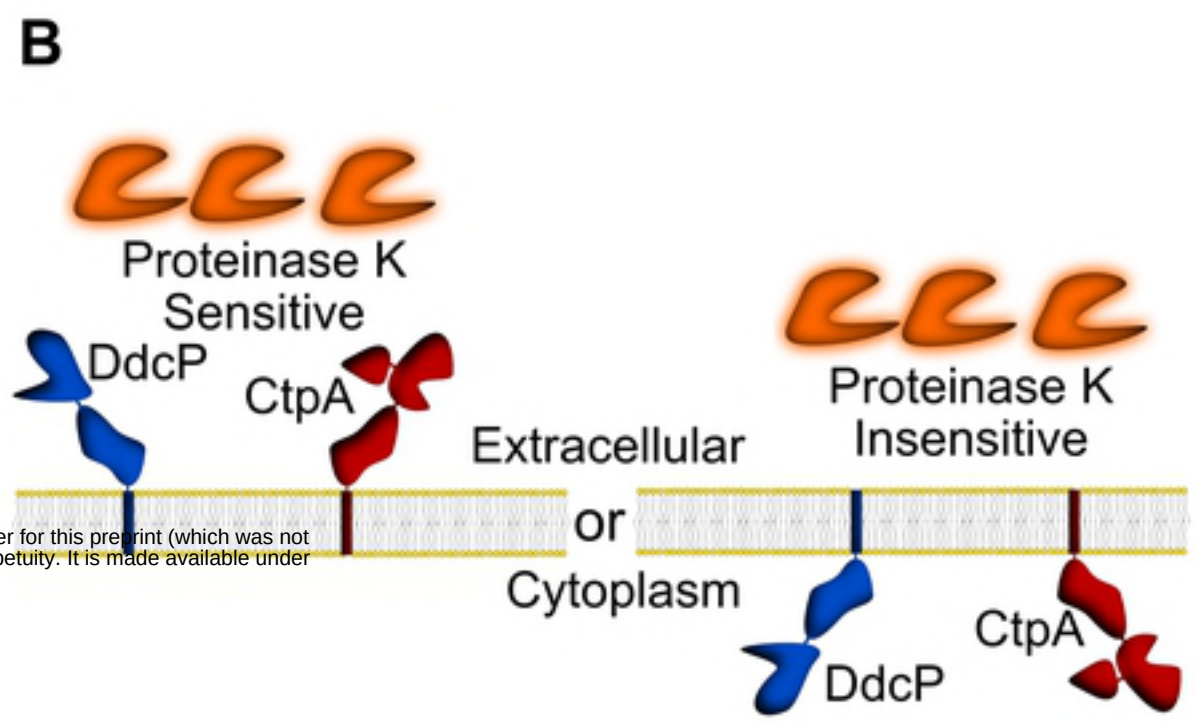

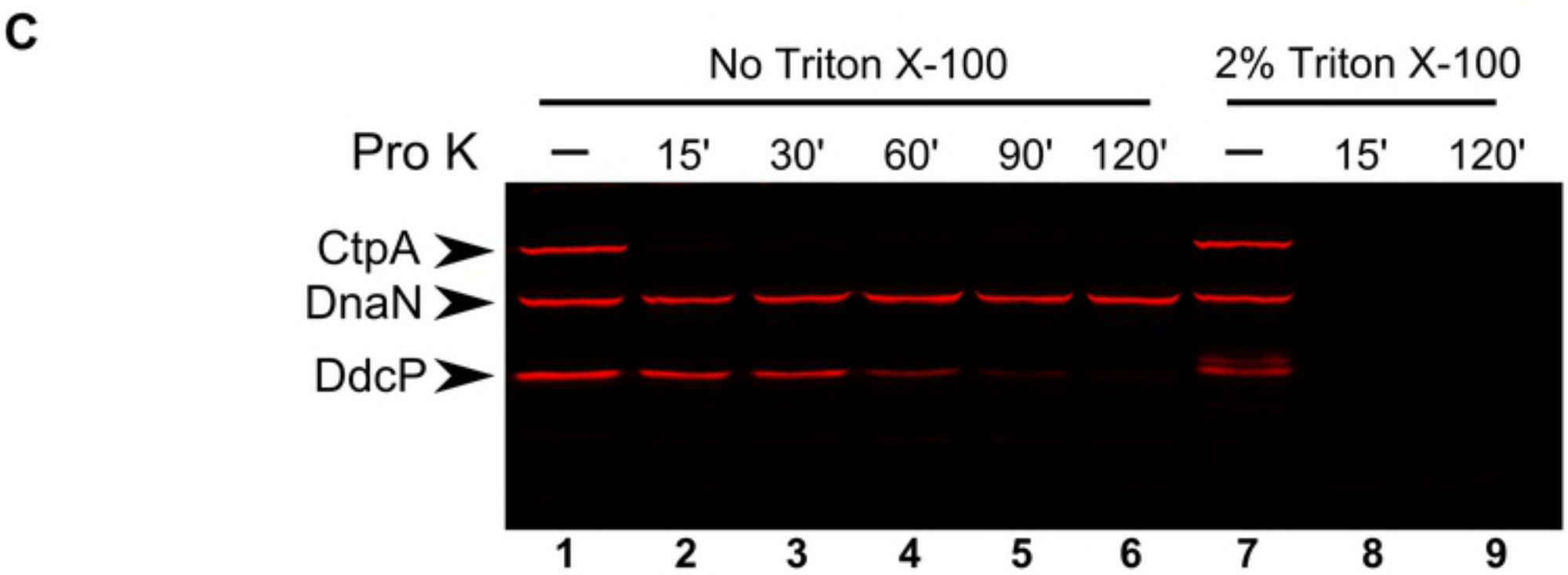

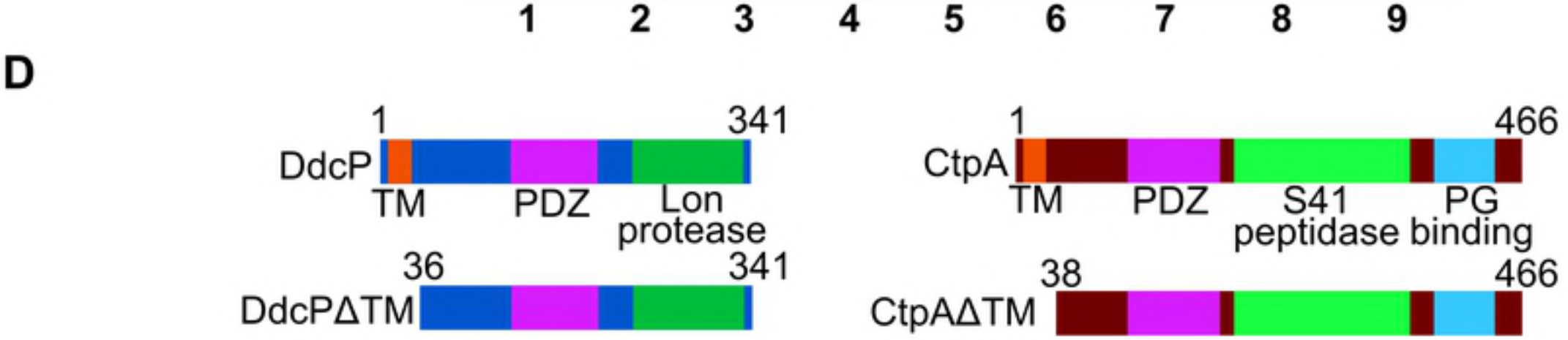

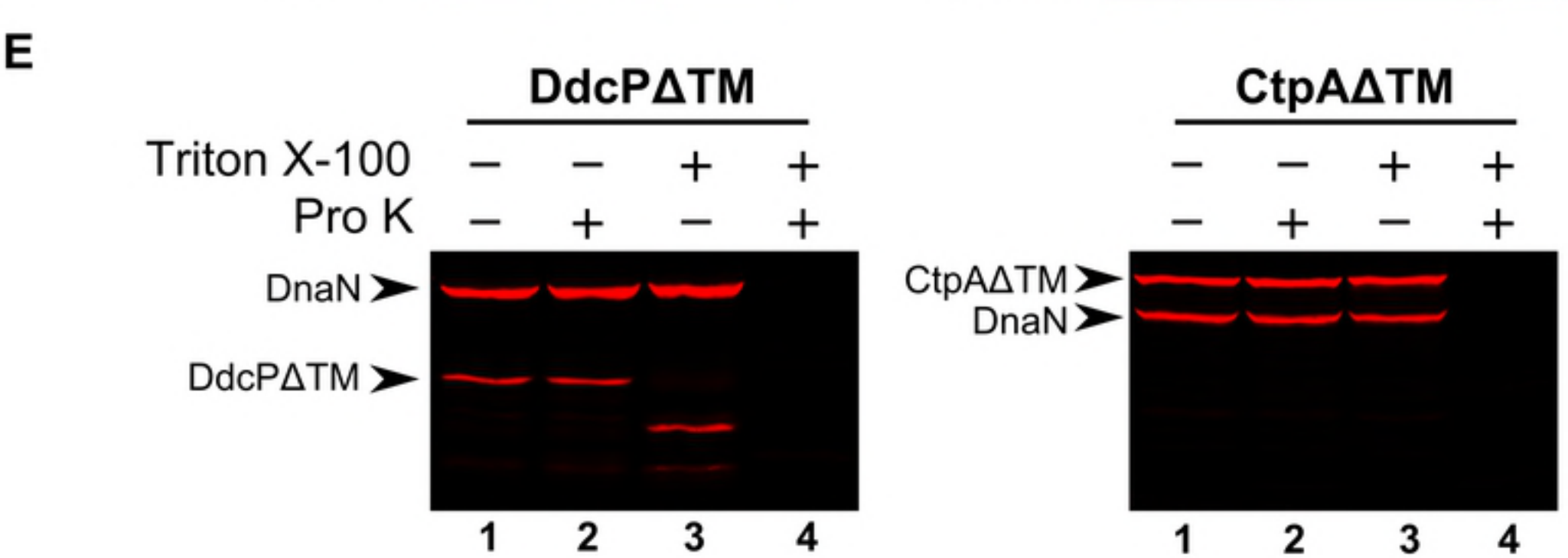

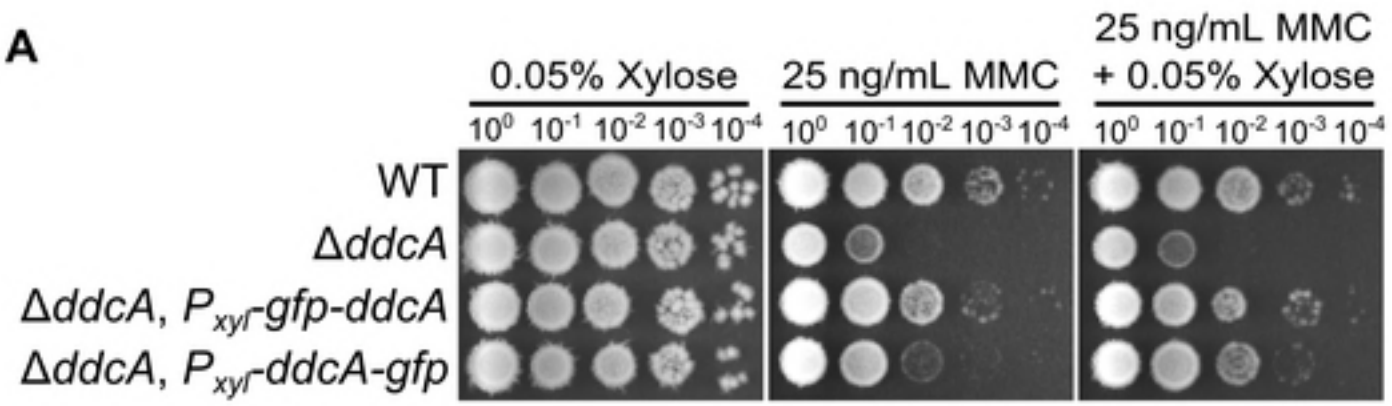

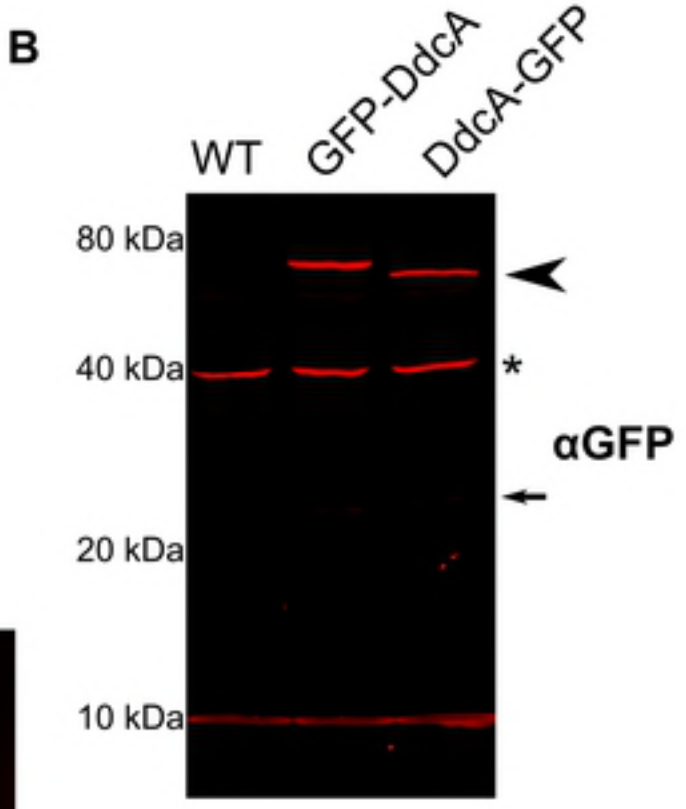

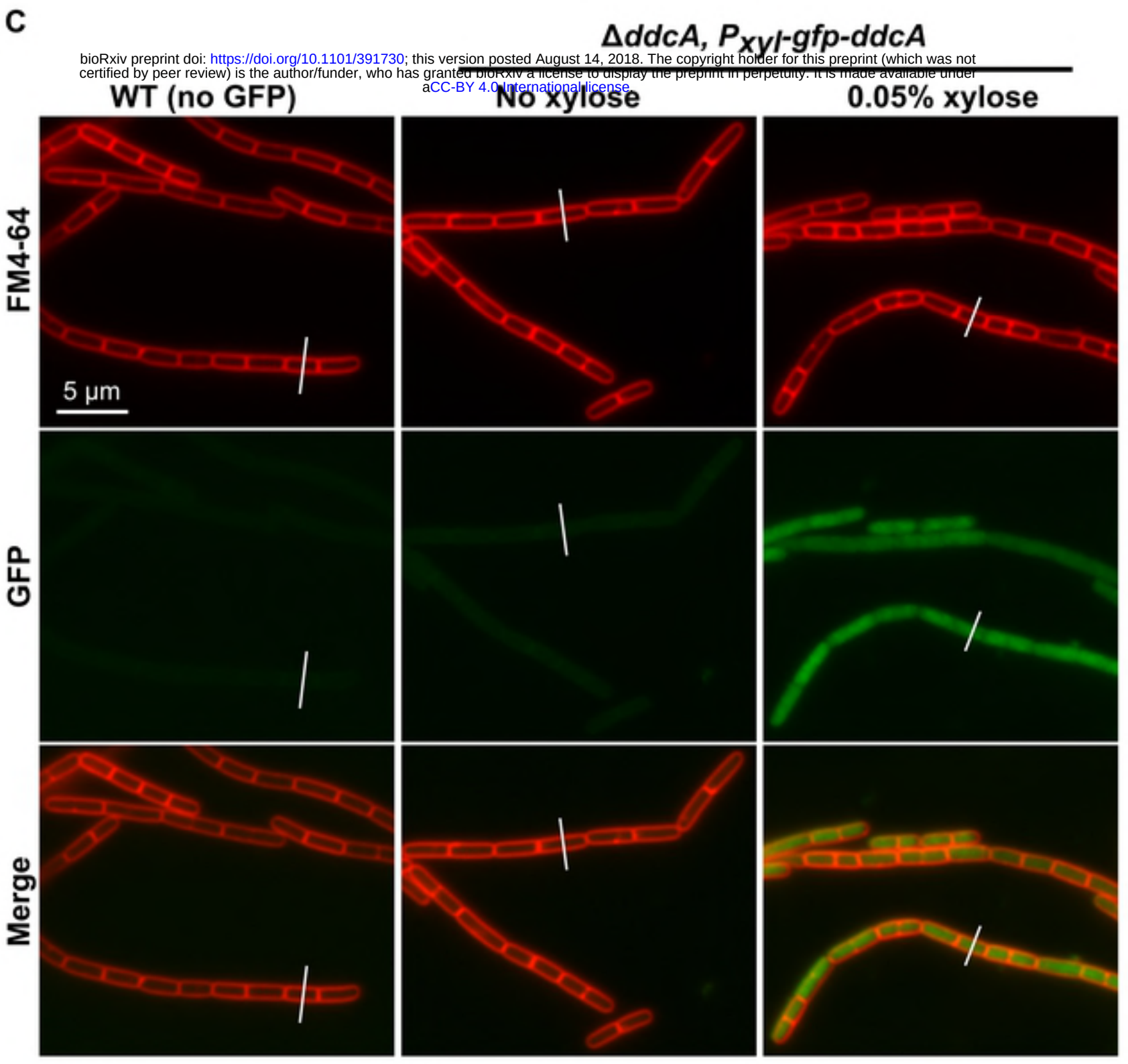

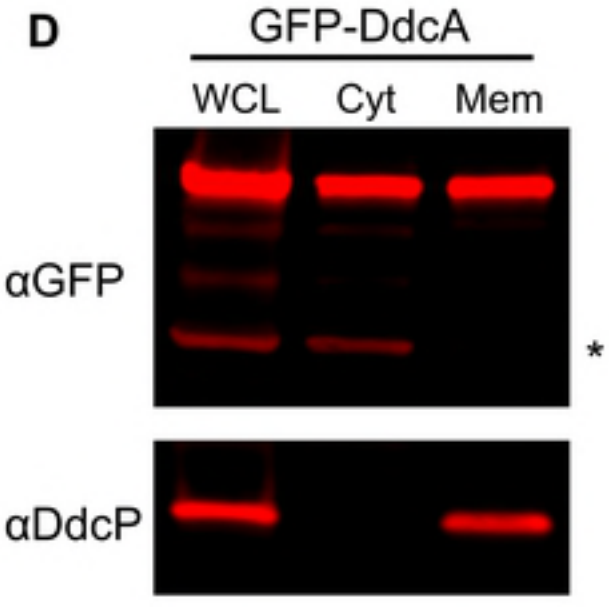

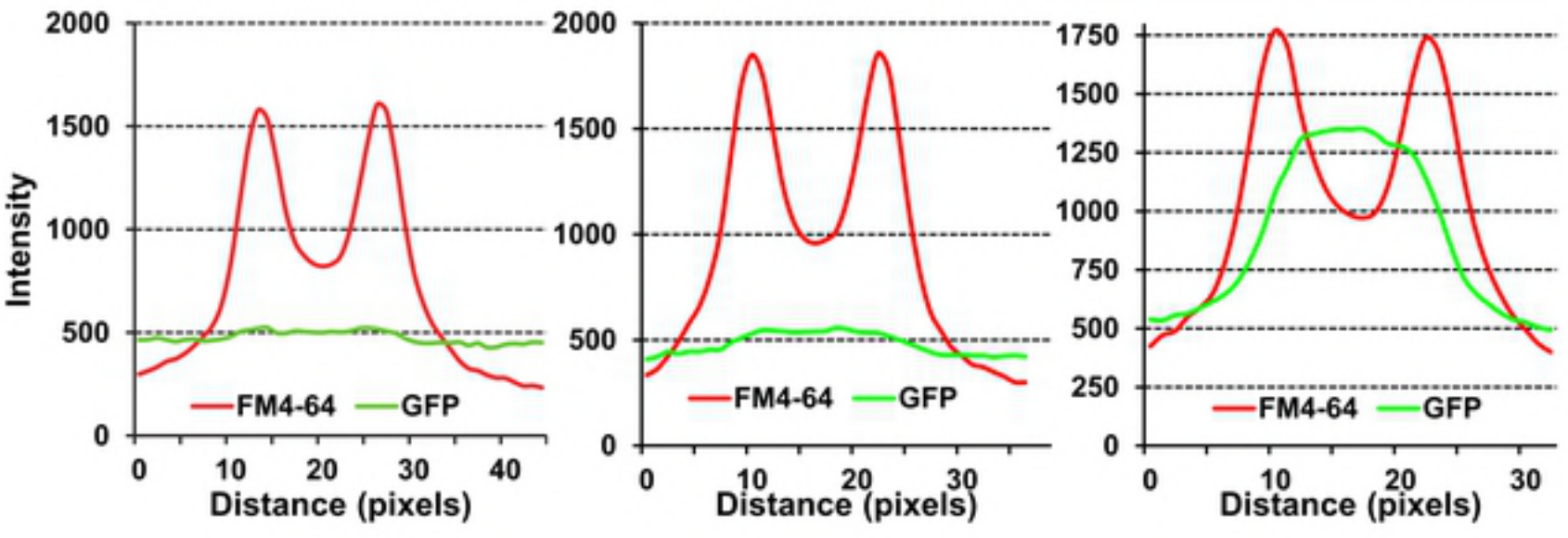

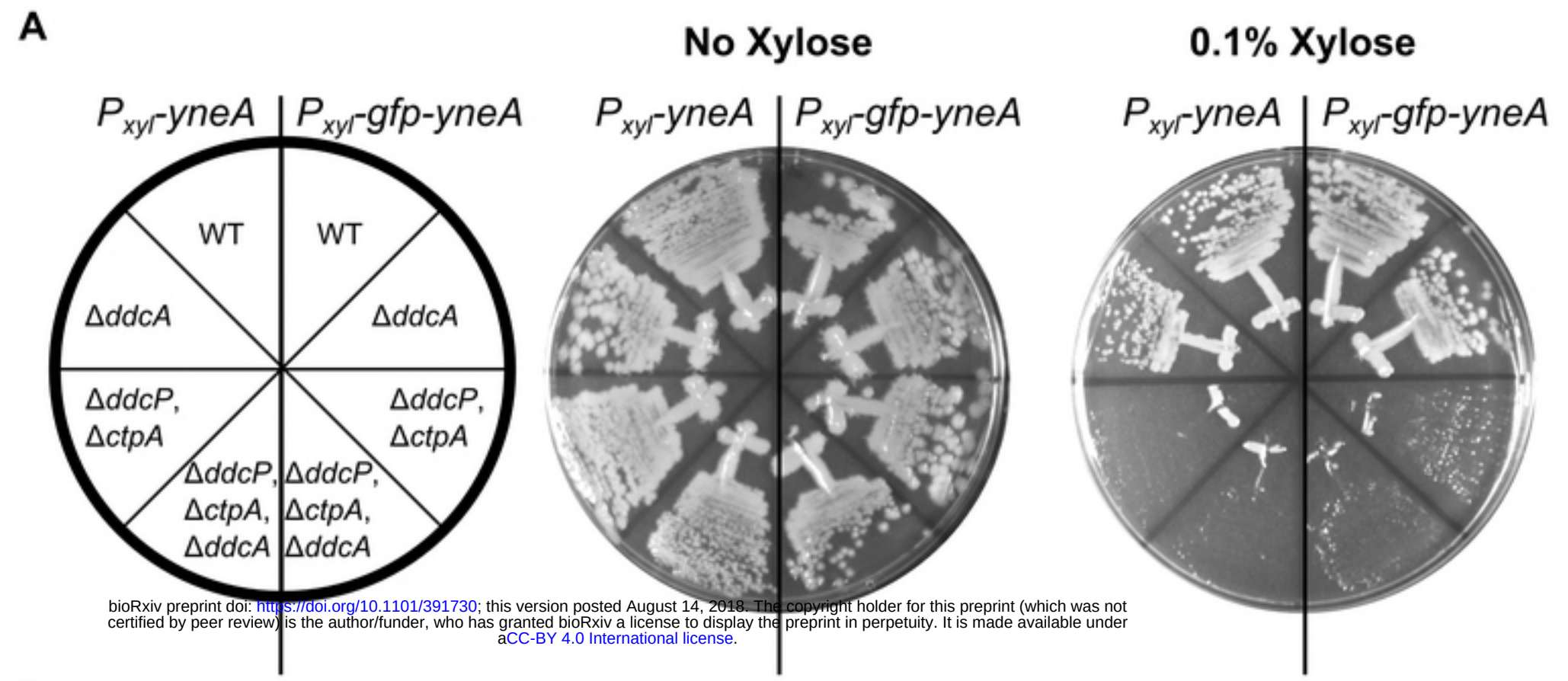

SOS OFF

LexA

DNA repair

Checkpoint

DNA damage &
SOS activation

RecA nucleo-
protein filament

SOS ON

DNA repair

Checkpoint

YneA overcomes
DdcA inhibition to
block cell division

SOS ON

DNA repair

Checkpoint

DNA Repair &
YneA is degraded

SOS OFF

DNA repair

Checkpoint

Cell Division

Legend

LexA

DdcP

CtpA

YneA

DdcA

Divisome

FtsZ